



Atypical resting-state functional brain connectivity in children with developmental coordination disorder

Dorine Van Dyck^{a,b,*}, Nicolas Deconinck^b, Alec Aeby^{b,d}, Simon Baijot^{b,d}, Nicolas Coquelet^a, Nicola Trotta^{a,c}, Antonin Rovai^{a,c}, Serge Goldman^{a,c}, Charline Urbain^{a,d}, Vincent Wens^{a,c}, Xavier De Tiège^{a,c}

^a Laboratoire de Cartographie Fonctionnelle du Cerveau (LCFC), ULB Neuroscience Institute (UNI), Université libre de Bruxelles (ULB), Brussels, Belgium

^b Department of Neurology, Hôpital Universitaire des Enfants Reine Fabiola (HUDERF), Université libre de Bruxelles (ULB), Brussels, Belgium

^c Clinics of Functional Neuroimaging, Service of Nuclear Medicine, CUB Hôpital Erasme, Université libre de Bruxelles (ULB), Brussels, Belgium

^d Neuropsychology and Functional Neuroimaging Research Group (UR2NF) at Center for Research in Cognition and Neurosciences (CRCN) and ULB Neurosciences Institute (UNI), Université libre de Bruxelles (ULB), Brussels, Belgium

ARTICLE INFO

Keywords:

Developmental coordination disorder
Motor disorder
Children
Resting-state functional connectivity
Magnetoencephalography

ABSTRACT

Children with developmental coordination disorder (DCD) present lower abilities to acquire and execute coordinated motor skills. DCD is frequently associated with visual perceptual (with or without motor component) impairments. This magnetoencephalography (MEG) study compares the brain resting-state functional connectivity (rsFC) and spectral power of children with and without DCD.

29 children with DCD and 28 typically developing (TD) peers underwent 2×5 min of resting-state MEG. Band-limited power envelope correlation and spectral power were compared between groups using a functional connectome of 59 nodes from eight resting-state networks. Correlation coefficients were calculated between fine and gross motor activity, visual perceptual and visuomotor abilities measures on the one hand, and brain rsFC and spectral power on the other hand. Nonparametric statistics were used.

Significantly higher rsFC between nodes of the visual, attentional, frontoparietal, default-mode and cerebellar networks was observed in the alpha (maximum statistics, $p = .0012$) and the low beta ($p = .0002$) bands in children with DCD compared to TD peers. Lower visuomotor performance (copying figures) was associated with stronger interhemispheric rsFC within sensorimotor areas and power in the cerebellum (right lobule VIII).

Children with DCD showed increased rsFC mainly in the dorsal extrastriate visual brain system and the cerebellum. However, this increase was not associated with their coordinated motor/visual perceptual abilities. This enhanced functional brain connectivity could thus reflect a characteristic brain trait of children with DCD compared to their TD peers. Moreover, an interhemispheric compensatory process might be at play to perform visuomotor task within the normative range.

1. Introduction

Developmental Coordination Disorder (DCD) is a neurodevelopmental disorder characterized by lower coordinated motor skills compared with typically developing (TD) peers (American Psychiatric Association, 2013). It impacts the daily living of ~ 5–6% of school-aged children from the early developmental period and is not better explained

by any medical condition affecting motor abilities. Motor difficulties refer mainly to postural control, motor learning and sensorimotor coordination (Geuze, 2005). The etiology of the disorder is still largely unknown but atypical brain functioning is considered as one of the main hypotheses (for reviews, see Biotteau et al., 2016; Fuelscher et al., 2018; Hyde et al., 2019).

Functional neuroimaging studies have been performed to unravel the

Abbreviations: ADHD, attention deficit hyperactivity disorder; DCD, developmental coordination disorder; DMN, default mode network; fMRI, functional magnetic resonance imaging; MABC-2, Movement Assessment Battery for children, 2nd edition; MEG, magnetoencephalography; PCC, posterior cingulate cortex; rsFC, resting state brain functional connectivity; RSNs, resting-state networks; TD, typically developing.

* Corresponding author at: Laboratoire de Cartographie fonctionnelle du Cerveau, Route de Lennik 808, CP 552/25, 1070 Brussels, Belgium.

E-mail address: Dorine.van.dyck@ulb.be (D. Van Dyck).

<https://doi.org/10.1016/j.nicl.2021.102928>

Received 8 September 2021; Received in revised form 6 December 2021; Accepted 22 December 2021

Available online 23 December 2021

2213-1582/© 2021 The Authors.

Published by Elsevier Inc.

This is an open access article under the CC BY-NC-ND license

(<http://creativecommons.org/licenses/by-nc-nd/4.0/>).

neural correlates of DCD. A limited number of task-based functional magnetic resonance imaging (fMRI) studies have been conducted. They evidenced modulations in blood oxygen level dependent (BOLD) signal in children with DCD compared with TD peers over brain regions involved in low- or high-level sensorimotor processes (with inconsistencies between studies, either decrease or increase in BOLD signal). These brain regions included the prefrontal areas (inferior, middle and superior gyri), the primary sensorimotor cortices, the posterior parietal cortex, the precuneus, the posterior cingulate cortex (PCC), the cerebellum (lobule VI, IX and crus I) and the basal ganglia (Debrabant et al., 2013; Licari et al., 2015; Reynolds et al., 2015a; Reynolds et al., 2019; Thornton et al., 2018; Zwicker et al., 2010; Zwicker et al., 2011). Increase in BOLD signal was also observed in the dorsolateral prefrontal cortex of children with DCD during tasks assessing executive functions, frequently impaired in DCD (Stroop and Wisconsin card sorting test, Koch et al., 2018). Atypical functional brain integration was found during motor tasks in children with DCD based on fMRI (Querne et al., 2008) and electroencephalographic (EEG) recordings (Blais et al., 2018; de Castelnau et al., 2008). These studies demonstrated the existence of atypical intra- or interhemispheric functional connectivity between these sensorimotor brain areas in children with DCD compared with TD children.

The apparent inconsistencies within this sparse functional neuroimaging literature can be explained by methodological differences between studies such as the tasks used to assess performance (e.g., finger tapping, tracing, or Go-NoGo) or the heterogeneity of the participants (e.g., presence/absence of associated disorders, variability of the age range, severity of the motor impairments, cut-off regarding the motor abilities of the TD children; Biotteau et al., 2016). One way to avoid task-related confound or performance bias is to study functional brain connectivity at rest (Deco and Corbetta, 2011). Resting-state functional brain connectivity (rsFC) reflects the neural communication between distant brain regions and allows to unravel similar functional brain networks as during task performance (Fox and Raichle, 2007; Smith et al., 2009). These functional networks underlie several specific low-level (e.g., visual, auditory or sensorimotor networks) or high-level (e.g., default-mode network (DMN), attentional, fronto-parietal networks) neural networks. To the best of our knowledge, only four resting-state fMRI studies have been conducted in children with DCD. In the first two, based on *a priori* hypotheses, authors measured rsFC between the left primary motor (M1) cortex (i.e., seed region) and the rest of the brain (McLeod et al., 2014; McLeod et al., 2016). Decreased rsFC was found in children with DCD between the seed and several cortico-subcortical regions involved in motor and sensorimotor processing (bilateral inferior frontal gyri, insular cortices, superior temporal gyri, right supramarginal gyrus, frontal operculum cortex and basal ganglia). A similar *a priori* approach showed abnormalities (i.e., stronger rsFC) in motor-related cortico-cerebellar connections and cortico-striatal connections mapping onto posterior parietal cortex in children with DCD (Cignetti et al., 2020). The fourth study identified the resting-state networks (RSNs) using a data-driven approach (i.e., independent component analysis, ICA) to explore functional brain connectivity without any *a priori* (Rinat et al., 2020). Using this approach, reduced rsFC between the sensorimotor network and the precuneus, the PCC and the left posterior middle temporal gyrus was observed in children with DCD (with or without concurrent attention deficit hyperactivity disorder, ADHD) compared to their TD peers. These atypical functional brain connectivity patterns were considered as the neural correlates of motor difficulties in DCD considering the involvement of those connections in motor learning, action-related information or processing (e.g., Cavanna and Trimble, 2006; Leech and Sharp, 2014; Papeo et al., 2015). The frequent occurrence of associated neurodevelopmental disorders such as ADHD, developmental language disorder, or developmental dyslexia combined with the heterogeneity of symptoms encountered in children with DCD (Dewey et al., 2002; Visser, 2003) can also explain the discrepancies observed in previous functional neuroimaging studies. ADHD

is characterized by deficits in attention, impulsivity or hyperactivity (American Psychiatric Association, 2013) and is co-occurring with DCD in up to 50% of the cases (Kadesjö and Gillberg, 1998). Hence, controlling for ADHD symptoms while investigating DCD pathophysiology may enable to clarify the specific characteristics associated to DCD (Van Dyck et al., Under review).

Beside fine and gross motor activity impairments, children with DCD also frequently present impairments in non-motor domains such as visual-perceptual abilities (Cheng et al., 2014; Tsai et al., 2008), visuospatial short-term memory (Alloway et al., 2009; Tsai et al., 2012) or executive functions (Leonard et al., 2015; Wilson et al., 2020). These alterations are not present in the entire DCD population (Tsai et al., 2008) but are part of the persisting symptoms of children with DCD (Bernardi et al., 2018; Wilson et al., 2020). These observations led to the assumption that several clinical subtypes can be described in DCD, with a substantial proportion of children presenting a subtype characterized by visual perceptual and visuomotor impairments (Hoare, 1994; Vaivre-Douret et al., 2011). Alterations within occipito-temporal and occipito-parietal brain circuits could therefore be expected based on the reported alterations in visual-perceptual abilities and action-oriented visual function (Hutchison and Gallivan, 2018; Rizzolatti and Matelli, 2003; Tsai et al., 2008). Still, in the data-driven resting-state fMRI study (Rinat et al., 2020), the visual network was excluded from comparison analyses as the ocular behavior of the participants was not controlled (i.e., eyes open/closed).

In this study, we used MEG to investigate the changes in resting-state functional brain architecture in children with DCD compared with their TD peers, while controlling for ADHD symptoms. MEG was preferred over EEG as it has been shown to better capture the interhemispheric rsFC within the sensorimotor network (Van Dyck et al., 2020). We used band-limited power-envelope correlation as a measure of rsFC as it allows to reproduce similar RSNs than those first highlighted using fMRI (e.g., low-level RSNs such as the sensorimotor, auditory and visual networks; or high-level RSNs such as the default mode, frontoparietal and dorsal attentional networks; Brookes et al., 2011; de Pasquale et al., 2010; Hipp et al., 2012; Wens et al., 2014). Although MEG RSNs are typically blurrier than fMRI RSNs due to the limited spatial resolution of MEG, a large number of independent studies have successfully discriminated between these different RSNs, in particular thanks to methodological developments on spatial leakage correction (Brookes et al., 2012; Hipp et al., 2012; Wens et al., 2015). Compared with fMRI, MEG has the advantage of providing direct information about neural activity, while allowing to investigate similar RSNs in a spectrally-resolved way thanks to its excellent temporal resolution (about the millisecond). Practically, rsFC was estimated using a comprehensive parcellation of the human brain (i.e., a connectome) into distinct RSNs. The visual network was included here as we controlled for several parameters related to ocular behavior during resting-state recordings (e.g., video-monitoring during MEG recordings, measure of the quantity of eye blinks and control for the arousal state based on alpha band power; Barry et al., 2007). Children also underwent a comprehensive motor and neuropsychological assessment. We expected to find (i) altered spectral power and rsFC within the sensorimotor and visual networks in children with DCD compared to TD peers, and (ii) associations between the severity of spectral power and rsFC changes within the sensorimotor/visual networks and those of motor/visual perceptual (with or without motor component) impairments in children with DCD.

2. Methods

2.1. Participants

We recruited 87 children with and without DCD aged between 7 and 11 years old. As depicted in Fig. 1, 30 participants were excluded from the study: 13 did not fulfill the inclusion criteria detailed below (6 DCD and 7 TD), 9 due to excessive movements or distance between head and

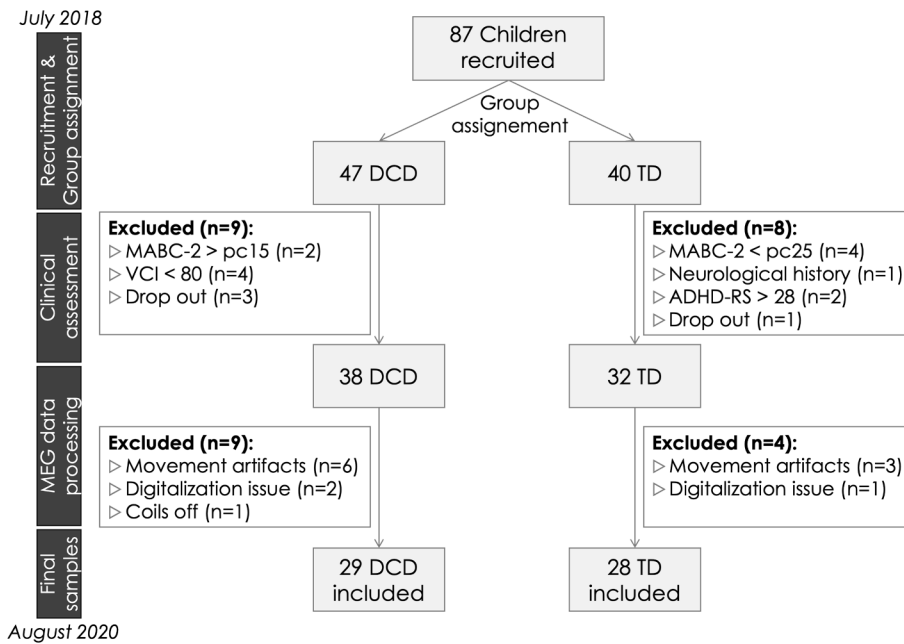


Fig. 1. Participant enrollment in the study and exclusion following the different stages of the experiment: 13 participants did not fulfill the inclusion/exclusion criteria, 4 dropped out of the study, and 13 were excluded due to MEG-related issues (excessive movement artifacts, important distance between head and sensors during MEG recordings, movements during head digitalization or a head position coil coming off the head). Abbreviations: DCD = Developmental Coordination Disorder; TD = Typical Development; MABC-2 = Movement Assessment Battery for Children, 2nd ed.; pc = percentile; VCI = Verbal Comprehension Index of the Wechsler Intelligence Scale for Children, 5th ed.; ADHD-RS = Attentional Deficit Hyperactivity Disorder Rating Scale IV; MEG = Magnetoencephalography.

sensors during MEG recordings (6 DCD and 3 TD), 3 due to excessive movements during head digitalization (2 DCD and 1 TD), one (1 DCD) due to a head position coil coming off the head (see section 2.3.1. *MEG and MRI data acquisition* for further details) and 4 who dropped out of the study (3 DCD and 1 TD). The final sample was therefore composed of 29 children with DCD (3 females and 26 males, mean age \pm SD: 9.74 ± 1.53 years) and 28 children with TD (12 females and 16 males, mean age \pm SD: 10.03 ± 1.33 years).

Children with DCD had to meet the four diagnostic criteria of the DSM-5 to be included in the study (American Psychiatric Association, 2013), assessed as follow : (i) global score equal or below the percentile 15th at the French version of the Movement Assessment Battery for children, 2nd edition (MABC-2, measure of the motor abilities; Henderson et al., 2007; Marquet-Doléac et al., 2016), (ii) score in the suspected or indicative range of DCD on the DCD-Q (measure of the impact of motor difficulties on the child's life; Martini et al., 2011), (iii) onset of symptoms in the early developmental period as assessed through a short parental anamnesis, and (iv) absence of neurological disorder assessed with a short parental anamnesis and through the medical file when available, or intellectual disability with the verbal comprehension index of the WISC-V (Wechsler, 2016). Children with DCD included in the study presented severe ($n = 18$; MABC-2 percentile \leq 5th) to moderate ($n = 11$; percentile 6–15th) motor impairment. Children with TD were included if they did not present any history of motor difficulties, their MABC-2 score was equal or above the percentile 25th, the DCD-Q was not indicative of a (suspected) DCD and if they had none of the following exclusion criteria.

Children from both groups were excluded from the study if they presented any intellectual disability (assessed with the WISC-V Verbal Comprehension Index < 80 ; Wechsler, 2016), autism spectrum disorder, history of psychiatric or neurological disorder, or were born very preterm (< 33 weeks gestational age; all controlled through a short parental anamnesis). The verbal comprehension index was chosen instead of total IQ as motor difficulties of children with DCD can have a deleterious impact on other IQ indices such as processing speed (Sumner et al., 2016). Moreover, TD children should not present any neurodevelopmental disability (controlled through short parental anamnesis and the parental questionnaire ADHD-RS-IV, score > 28 being indicative of ADHD; DuPaul et al., 1998). In children with DCD, concurrent ADHD diagnosis was not an exclusion criterion ($n = 17$), as

neurodevelopmental comorbidities are frequent in DCD (Dewey, 2018; Piek and Dyck, 2004). ADHD diagnosis was assessed according to DSM-5 criteria (American Psychiatric Association, 2013) by a multidisciplinary team including pediatric neurologists and neuropsychologists. Methylphenidate medication for ADHD ($n = 9$) was interrupted at least 24 h before the experiment. In all participants, the severity of ADHD symptoms was measured through the ADHD-RS-IV parental questionnaire (DuPaul et al., 1998), assessing the main symptoms of inattention and hyperactivity/impulsivity following DSM criteria (American Psychiatric Association, 2013).

Children presenting DCD were recruited through neuropsychiatrists and health professionals' consultations ($n = 22$) as well as social media ($n = 5$) and primary schools ($n = 2$). Children from the TD group were recruited either through primary schools after receiving the approval of school authorities ($n = 2$), social media ($n = 7$) or acquaintances ($n = 19$) in the French-speaking part of Belgium. All participants participated in a longer experimental protocol, involving electroencephalography investigations (Van Dyck et al., 2020) and a procedural learning task (Van Dyck et al., 2021).

Written informed consents were obtained from all participants and their parents. The study was approved by local Ethics Committee of CUB Hôpital Erasme (Reference: P2018/179) and Hôpital Universitaire des Enfants Reine Fabiola (Brussels, Belgium).

2.2. Material and design

2.2.1. Experimental design

Participants underwent a clinical assessment and a MEG investigation (order counterbalanced between subjects) during one (TD = 23/28; DCD = 1/29), two (TD = 5/28; DCD = 19/29) or three (DCD = 9/29) different days to avoid fatigue effect (mainly within the month, except for five participants, due to difficulties to manage appointments [40, 58, 63 or 100 days between the first and last appointments] or to COVID-19 pandemic lock-down [147 days]).

During the MEG investigation, participants were first prepared for MEG acquisition (i.e., head position coils placement and head digitalization) while watching cartoons. They were then moved in the MEG chair and sat comfortably for two successive 5-min sessions of resting state. They were asked to sit as still as possible and to gaze at a picture of their favorite cartoon chosen beforehand, printed and displayed on a

wall at 2 m in front of them.

A structural brain magnetic resonance image (MRI) was finally acquired to enable MEG source reconstruction, either on the day of clinical assessment or that of MEG recording, but never before the MEG investigation.

Data acquisition was done at CUB Hôpital Erasme (Brussels, Belgium). Six children with DCD performed the clinical assessment at the Hôpital Universitaire des Enfants Reine Fabiola (Brussels, Belgium) with the same investigator.

2.2.2. Clinical assessment

All participants were initially screened for inclusion/exclusion criteria. A semi-structured interview with at least one parent and the child was conducted to learn more about the impact of motor difficulties on daily living and school productivity, any possible associated disorder or medical condition, medical and pregnancy history and the socio-economic status (SES). The latter was estimated with a double 6-point scale based on the addition of each 6-point scale for each parent's education level (SES lowest score = 2, highest score = 12; adapted from Largo et al., 1989). Laterality was assessed with the Edinburgh Handedness Inventory scale (Oldfield, 1971). Each participant underwent a comprehensive neuropsychological assessment comprising the evaluation of (1) visuo-perceptual abilities using visual closure subtest of the DTVP-2 (Hammill et al., 1993) and a bar orientation recognition test (Lacert, 1987); (2) visuomotor abilities using the eye-hand coordination and copying subtests of the DTVP-2 (Hammill et al., 1993); (3) visual constructional abilities using the block design subtest of WISC-V (Wechsler, 2016); (4) sensorimotor abilities using hand position imitation and motor sequences of NEPSY-II (Korkman et al., 2007); (5) visuospatial short-term memory with a block tapping test (Fournier and Albaret, 2013) and verbal working memory using backward digit span (WISC-V; Wechsler, 2016); (6) executive functions, more specifically cognitive inhibition with the difference between interference and denomination parts of a non-reader version of the Stroop test (Catale et al., 2014), motor inhibition with a Go-NoGo test (Zimmermann and Fimm, 2004), planning with a child-adapted version of Tower of London (Shallice, 1982), and flexibility with a Revised Wisconsin Card Sorting Test (Nelson, 1976); (7) attentional functions with the coefficient of variation of reaction times (alertness test; Zimmermann and Fimm, 2004).

The clinical assessment allowed to check the inclusion/exclusion criteria, characterize the clinical profile of children with DCD, and ultimately address possible associations between functional brain connectivity and clinical parameters. The order between tasks was counterbalanced between subjects.

2.3. Data acquisition and processing

2.3.1. MEG and MRI data acquisition

Participants' neuromagnetic activity was recorded (band-pass filter: 0.1–330 Hz, sampling rate: 1 kHz) using a 306-channel whole-scalp neuromagnetometer (TriuxTM, MEGIN, Croton Healthcare, Helsinki, Finland) installed in a light-weight magnetically shielded room (MaxshieldTM, MEGIN, Croton Healthcare, Helsinki, Finland; see De Tiege et al., 2008 for details) at the CUB Hôpital Erasme. Four head-tracking coils were placed on the subjects' head to monitor head position inside the MEG helmet. Their location relative to anatomical fiducials and at least 300 head-surface points were digitized prior to data acquisition using an electromagnetic tracker (Fastrack, Polhemus, Colchester, VT).

A high-resolution structural 3D T1-weighted brain MRI was acquired either on a 1.5 T MRI scanner (n = 33; Intera, Philips, Best, The Netherlands) or on a hybrid 3 T PET-MRI scanner (n = 21; Signa 3 T, General Electric Healthcare, Wisconsin, USA) installed at the CUB Hôpital Erasme. The MRI of 3 children was missing (due to excessive head motion, fear or following the parents' decision). A linear deformation of the structural images from another child's brain of roughly the

same age (to best match head-surface points) was thus used instead. These surrogate MRIs were obtained with the CPD toolbox (Myronenko and Song, 2010) embedded in FieldTrip (Donders Institute for Brain Cognition and Behaviour, Nijmegen, The Netherlands, RRID: SCR_004849; Oostenveld et al., 2011).

2.3.2. MEG data preprocessing

Environmental magnetic noise was suppressed and head movements were corrected using the temporal extension of the signal space separation algorithm (Taulu et al., 2005; correlation limit, 0.98; window length, 10 s; MaxfilterTM, Elekta Oy, Helsinki, Finland; version 2.2 with default parameters). Time periods contaminated by excessive movements or muscular artifacts were visually identified by inspection of the whole recorded signal and eliminated from subsequent analysis. Usage of ICA (FastICA algorithm with dimension reduction to 30 and hyperbolic tangent nonlinearity contrast; Vigario et al., 2000) of the band-pass filtered (1–40 Hz) MEG signals allowed to suppress remaining cardiac and ocular artifacts. Components corresponding to artifacts were visually identified and regressed out of the full-rank data (number of components removed from data, mean \pm SD [range]: DCD = 5.88 ± 1.69 [4–13]; TD = 5.27 ± 1.53 [3–10]). The cleaned MEG data were then filtered into four frequency bands (theta: 4–8 Hz; alpha: 8–12 Hz, low beta: 15–21 Hz, high beta: 21–30 Hz). The alpha and beta frequency bands were chosen as they support the power envelope coupling among low-level (e.g., sensorimotor, visual, auditory) and high-level (e.g., default-mode network (DMN), attentional networks, executive networks) electrophysiological RSNs, as well demonstrated both in healthy adults (Brookes et al., 2011; Coquelet et al., 2020; Hipp et al., 2012; Liu et al., 2017; Liu et al., 2018; Sjøgård et al., 2019; Wens et al., 2014) and in children (Van Dyck et al., 2020). The theta frequency band was also included as children tend to exhibit slower spontaneous rhythmic brain activity than adults (Rodríguez-Martínez et al., 2017).

2.3.3. MEG source reconstruction

The participants' brain MRI was preprocessed to compute the MEG forward model, necessary to proceed with MEG source reconstruction. The structural MRI was anatomically segmented using the FreeSurfer software (Martinos Center for Biomedical Imaging, Massachusetts, USA; RRID: SCR_001847; Fischl, 2012). MEG and structural MRI coordinate systems were coregistered manually using the digitized fiducial points for initial estimation and head-surface points for refinement (MriLab, MEGIN Croton Healthcare, Helsinki, Finland). A volumetric source grid (5 mm) was built with the Montreal Neurological Institute (MNI) template MRI and mapped on each subject's MRI using a non-linear deformation (SPM12, Wellcome Trust Centre for Neuroimaging, London, UK; RRID: SCR_007037; Ashburner and Friston, 1999). Three-dimensional dipole sources were then placed on each node of this grid. MEG forward model was finally computed on this source space using the one-layer boundary element method of the MNE-C suite (Martinos Centre for Biomedical Imaging, Massachusetts, USA; Gramfort et al., 2014).

Source activity was reconstructed in each of the considered frequency bands using minimum norm estimation (MNE; Dale and Sereno, 1993). The MEG noise covariance matrix was estimated based on 5 min MEG empty-room data recorded for each participant, preprocessed using signal space separation, and filtered in each frequency band. The MNE regularization parameter was set based on the consistency condition from Wens et al. (2015). The resulting three-dimensional dipole time series were projected on their direction of maximum variance (Sjøgård et al., 2019; Wens et al., 2014) and their analytic signal was obtained via Hilbert transformation. Nodes signals were extracted as pointwise signals at each node location.

2.3.4. Comparability of resting-state data between groups

Children's head size, their tendency to move inside the MEG helmet, as well as the different ocular behavior that participants can adopt

during the resting-state sessions may affect MEG recording quality. This could potentially lead to MEG signal differences between DCD and TD groups unrelated to actual brain functioning. MEG data quality was therefore assessed in both groups to ensure their comparability before turning to rsFC estimation. We measured for each participant and each resting-state session: (i) the quantity of eye blinks, estimated by counting the number of blinks identified by signal peaks exceeding signal mean $\pm 1.65SD$ in the independent components corresponding to ocular artifacts; (ii) the total MEG data duration after removing bad time periods; (iii) the number of artefactual components identified; (iv) the alpha-band power averaged across all the occipital nodes (i.e., nodes part of the visual network; see the following section 2.3.5. *Functional connectivity estimation*) as an indicator of participants' arousal state (Barry et al., 2007). In case of significant differences in data duration, MEG data were cut so as to ensure similar duration on average between DCD and TD children.

2.3.5. Functional connectivity estimation

The rsFC was quantified between two source time courses as their envelope correlation (Brookes et al., 2011; de Pasquale et al., 2010; Hipp et al., 2012; Wens et al., 2014) after signal orthogonalization in order to correct for spatial leakage (Brookes et al., 2012). Envelopes were low-pass filtered below 1 Hz and their temporal correlation was then calculated over the whole data duration (i.e., excluding time periods marked as bad; Wens et al., 2014; Wens et al., 2015).

The rsFC was estimated within a connectome based on a parcellation of the human brain into 59 major nodes (see Fig. 2 for an overview of their location) of 8 well-known RSNs: default-mode network (DMN), dorsal attentional network (DAN), language network (LAN), sensorimotor network (SMN), ventral attentional network (VAN), visual network (VN) taken from de Pasquale et al. (2012), frontoparietal network (FPN; obtained from Della Penna et al., 2019), and cerebellar network (Naeije et al., 2020). The frontoparietal and cerebellar nodes were added to the parcellation of de Pasquale et al. (2012) given the assumptions (Bo and Lee, 2013; Zwicker et al., 2009) and evidence (Debrabant et al., 2013; Querne et al., 2008; Licari et al., 2015; Reynolds et al., 2015a; Reynolds et al., 2019; Thornton et al., 2018; Zwicker et al., 2010) regarding the involvement of the cerebellum, parietal and frontal lobes in DCD pathophysiology.

The use of this connectome resulted in a 59-by-59 rsFC matrix per subject and frequency band, which was further symmetrized by averaging them with their transpose as in Hipp et al. (2012) to avoid possible asymmetries emerging after pairwise orthogonalization (for a discussion, see Coquelet et al., 2020). We also estimated the signal power variance at each node, with noise standardization to correct for the

depth bias (Pascual-Marqui, 2002). Node power was introduced in as covariate of no interest in subsequent statistical models to avoid rsFC group differences solely due to concomitant power differences (Muthukumaraswamy and Singh, 2011). The depth bias in node variance estimation was corrected beforehand using noise standardization (Pascual-Marqui, 2002). Finally, the rsFC matrices corresponding to the two resting-state recordings were averaged to improve the stability of rsFC estimation (Liuzzi et al., 2017).

2.4. Data analyses

2.4.1. Statistical analyses on behavioral measures from clinical assessment

Before comparing both groups on the behavioral and clinical measures, participants deviating from >3 median absolute deviation in each behavioral measure were considered as outliers for each group of participants and removed from the comparison analysis on the concerned measure (Leys et al., 2013). Questionnaires, motor and neuropsychological assessment scores were compared between children with DCD and TD using two-tailed unpaired *t* tests. Significance level was set to $p < .002$, Bonferroni corrected for the number of scores ($p < .05/22$). Results in visual perceptual and visuomotor assessment from both samples were also compared to normative data to describe the proportion of children in each group presenting impairment in each test.

2.4.2. Comparability of resting-state MEG data between groups of participants

The quantity of eye blinks, total MEG data duration after removing bad time periods, number of artefactual components identified, and occipital alpha-band power were averaged across the two resting-state sessions and compared statistically between the two groups using unpaired *t* tests.

2.4.3. Resting-state functional connectivity and spectral power differences between children with DCD and TD

To investigate group differences in the functional connectome, we contrasted DCD and TD node power and rsFC group-averaged data using mass-univariate unpaired *t* tests (one per connection and frequency band), implemented as a regression model to incorporate covariates of no interest. Specifically, the contrast was measured using a covariate of interest labelling group dependence. Five variables were introduced as covariates of no interest for comparison analyses performed on rsFC and spectral power: sex, age, the severity of the ADHD symptoms (score at the parental questionnaire ADHD-RS-IV; DuPaul et al., 1998), the verbal comprehension index (Wechsler, 2016) and laterality (score at the Edinburgh questionnaire; Oldfield, 1971). For rsFC, node power at the

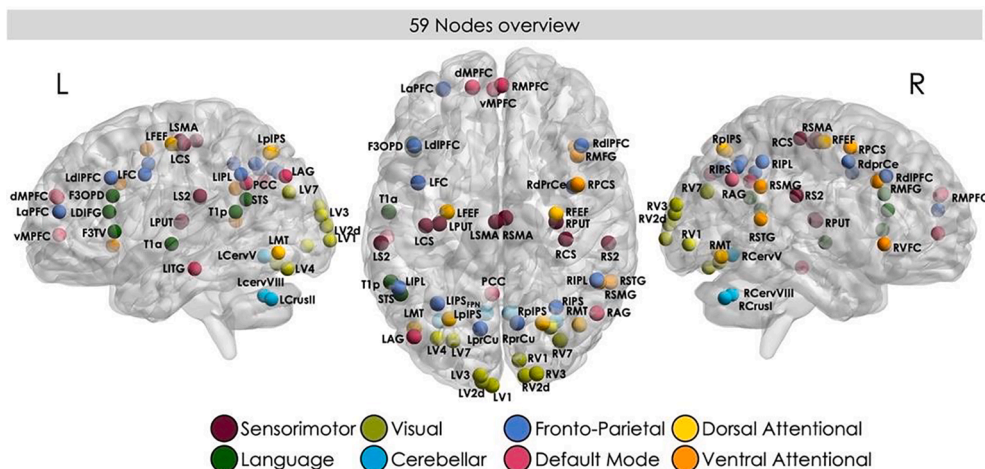


Fig. 2. Overview of the location of the 59 nodes belonging to 8 resting-state networks used for the connectome analysis. Brain figures were realized using the BrainNet viewer (Xia et al., 2013). L = left hemisphere, R = right hemisphere.

two nodes of a connection was additionally introduced as covariates of no interest to exclude possible rsFC group differences concomitant to node power changes (Muthukumaraswamy and Singh, 2011).

Contrast significance was established using non-parametric testing based on a maximum statistic (Nichols and Holmes, 2002). Here, the maximum statistic corresponded to maximum (taken over all 1711 connections) absolute value of the regression coefficient corresponding to the group contrast factor. Taking the absolute value allowed to design a two-sided test, and taking the maximum allowed to correct for the multiple comparisons associated with the number of connections in the connectome. More specifically, assuming the absence of between-group difference, we generated 4000 null samples of the group contrast coefficient by randomly permuting the group label ("DCD" vs "TD") of each subject in the covariate of interest (while keeping covariates of no interest fixed) before constructing the regression model. Importantly, keeping covariates of no interest fixed while permuting the covariate of interest (i.e., group label) preserved the relationship between the connectivity or spectral power weights and the covariates of no interest, so their effects were still correctly controlled in permuted data. We retained the maximum group contrast coefficient across all connections of the connectome, and the 95th percentile of the resulting distribution of maxima yielded the two-tailed significance threshold for the group contrast coefficients at $p < .0125$ (i.e., 0.05 further Bonferroni corrected for 4 frequency bands) with full control of the false positive rate (Nichols and Holmes, 2002). P -values were obtained from each null distribution as the fraction of null samples above the observed (non-permuted) maximum statistic.

Of note, these statistical analyses were performed separately for each of the four frequency bands, instead of using a single maximum statistics taken over all four connectomes. While this idea would be theoretically justified to correct for the frequency band factor and avoid our usage of Bonferroni correction, it has practical limitations. Indeed, one issue with the maximum statistic is that large significant effects can overshadow smaller effects, as strong effects are generally associated with large variance and may dominate the variance of the maximum statistic (Nichols and Holmes, 2002). Separating the maximum statistics according to the frequency band allows to avoid the issue that different frequency bands typically exhibit different effect sizes.

2.4.4. Relationship between resting-state functional connectivity, spectral power and behavioral measures

Being particularly interested in motor and visual perceptual difficulties with or without motor component in children with DCD, we selected 10 subtests assessing these functions to perform correlation analyses: MABC2 (global score and 3 subscales scores), visual closure, eye-hand coordination, copying (DTVP-2; Hammill et al., 1993), bar orientation recognition (Lacert, 1987), the Corsi's block tapping test (Fournier and Albaret, 2013) and the block design subtest of WISC-V (Wechsler, 2016). Outliers in any behavioral measure were removed from the correlation analysis involving this behavioral measure.

Correlations between rsFC and these behavioral measures were sought within the DCD group only, for each connection in the connectome and each frequency band, via mass-univariate regression analyses similar to those described for the contrast, with the same set of covariates of no interest, except that behavioral measures were used as covariates of interest instead of the group label factor. A positive (or negative) regression coefficient between a behavioral measure score and electrophysiological measures indicated that a stronger (or lower) rsFC of the corresponding connection or a stronger (or lower) power at the corresponding node was associated with a better (or lower) performance in the task. Given that the score of bar orientation recognition (Lacert, 1987) represents the amount of errors, a positive (or negative) regression coefficient indicated that a stronger (or lower) rsFC of the corresponding connection or a stronger (or lower) power at the corresponding node was associated with a lower (or better) performance in the task.

Statistical significance of regression coefficients was assessed in a

way similar to the group contrast regression model, with the only difference that subjects ordering was randomly permuted within the DCD group in the behavioral covariates (but not in the covariates of no interest) before regression modeling and extracting the maximum of their absolute regression coefficient over all connections.

3. Results

3.1. Behavioral results

Demographic and clinical data are reported in Table 1. Several outliers were detected in the clinical assessment using the 3 median absolute deviation measure (Leys et al., 2013) and removed from behavioral data ($n/10$ subtests [range of n outliers] : DCD = 2/10 subtests [2–3]; TD = 2/10 subtests [1–3]) before performing the comparison analysis on this specific measure. Children with DCD presented, as a group, inferior performance compared to their TD peers in fine and gross motor activity and sensorimotor functions but also working memory and visual perceptual/visuospatial abilities, with and without motor component. We then compared the data with the normative data available in the different standardized tests according to the age of the child to characterize the proportion of children in our sample presenting impairments in the visual perceptual / visuospatial abilities, visuomotor abilities and visuospatial short-term memory (see Fig. 3). A total of 65.5% of our DCD sample ($n = 19$) against 0% of the TD sample ($n = 0$) presented an impairment in at least one of these areas. Regarding the subtests taken individually, 41.4% ($n = 12$) of children with DCD presented performance below the 5th percentile (set at the false-positive rate, Godefroy et al., 2014; or 1.65 standard deviation from the mean) in visual closure, 24.1% ($n = 7$) in bar orientation recognition and in eye-hand coordination, 6.9% ($n = 2$) in the block design' subtest of WISC-V, 10.3% ($n = 3$) in visuospatial short-term memory and 0% ($n = 0$) in copying figures.

3.2. Comparability of resting-state data between groups

A significant group difference was found on the averaged recording time (mean \pm SD: DCD = 293 s \pm 12.3, TD = 299 s \pm 3.59; $t(55) = -2.48$; $p = .02$; $d = -0.65$) but not on the quantity of eye blinks ($p = .49$), the number of artefactual ICs removed ($p = .08$) or occipital alpha-band power ($p = .22$). To correct the inequality in recording duration between DCD and TD children, we removed the mean difference from the end of the MEG data for each child from the TD group (rest 1 = 6.945 s; rest 2 = 4.897 s).

3.3. Resting-state functional connectivity and spectral power differences between children with DCD and TD

Comparison analyses between groups revealed no significant difference at the level of node power (maximum statistics, all $ps > 0.07$). This is suggestive that no modification of spectral power should bias rsFC contrasts. Still, given that absence of significance does not equal absence of effect, node power was explicitly used as covariates of no interest in our rsFC analyses.

Comparison of rsFC showed significant differences between DCD and TD groups in the alpha (maximum statistics, threshold = 0.0545, $p = .00125$) and the low beta (threshold = 0.0318; $p = .00025$) bands (all other $ps > 0.0127$). Higher values of rsFC were found in children with DCD, mainly in parietal, occipital, temporal and cerebellar nodes involved in the visual, dorsal and ventral attentional, frontoparietal, default-mode and cerebellar networks (see Fig. 4 and Table 2 for further details). However, while looking at the specific brain regions involved in the significant between-group differences of rsFC, the results suggest that these differences are mainly located within the visual system (see Fig. 4). These nodes are then not further interpreted in terms of RSNS. The distribution of the null samples, the threshold and the maximum statistic value are provided in supplementary materials for both resting-

Table 1
Descriptive measures for demographic and clinical data.

	DCD (n = 29)	TD (n = 28)		p
Demographics and clinical characteristics				
Sex, n F/M	3/26	12/16	$\chi^2(1) = 7.77$	0.005*
Laterality, n R / L / A	23/4/2	26/2/0	$\chi^2(2) = 2.83$	0.24
Age (years)	9.74 ± 1.53	10.03 ± 1.34	t(55) = -0.77	0.44
Socioeconomic status	9.25 ± 1.96	10.9 ± 2.04	t(53) = -3.04	0.004*
Questionnaires				
DCD-Q	36.9 ± 12.00	65.3 ± 6.49	t(42.1) = -10.9 ^a	<0.001**
ADHD-RS	28.97 ± 11.08	12.21 ± 7.37	t(48.9) = 6.74 ^a	<0.001**
Pathological ADHD-RS score, yes/no	16/13	0/28	–	–
Fine and gross motor abilities				
MABC-2 (pc)	4.33 ± 3.96	51.68 ± 22.24	t(28.7) = -11.10 ^a	<0.001**
Manual Dexterity (SN)	4.14 ± 1.55	9.50 ± 2.49	t(45) = -9.73 ^a	<0.001**
Aiming and catching (SN)	7.17 ± 2.47	9.96 ± 2.50	t(55) = -4.24	<0.001**
Static-dynamic balance (SN)	6.21 ± 3.04	11.43 ± 1.43	t(40) = -8.35 ^a	<0.001**
Neuropsychological assessment				
VCI, intelligence score	105.72 ± 13.77	115.32 ± 12.50	t(55) = -2.75	0.008*
VC, visual-perceptual (correct trials) ^b	10.00 ± 5.84	18.00 ± 1.41	t(31.8) = -7.14 ^a	<0.001**
BO, visual-spatial perception (errors)	6.28 ± 4.47	3.46 ± 3.26	t(55) = 2.70	0.009*
EH, oculomotor coordination (score) ^b	156 ± 16.8	173.79 ± 6.47	t(33.4) = -5.29 ^a	<0.001**
COPY, visuomotor abilities (score) ^b	24 ± 5.29	34.1 ± 2.78	t(43) = -9.03 ^a	<0.001**
BD, visual constructional (score) ^b	8.12 ± 1.80	11.93 ± 2.43	t(49.6) = -6.58 ^a	<0.001**
IHP, sensorimotor (correct trials)	17.72 ± 3.93	22.00 ± 2.23	t(44.6) = -5.08 ^a	<0.001**
MMS, sensorimotor (score)	39.10 ± 6.20	48.11 ± 5.43	t(55) = -5.82	<0.001**
BTT, visual-spatial STM (max.)	4.72 ± 1.07	5.89 ± 1.10	t(55) = -4.07	<0.001**
BDS, working memory (max.)	3.38 ± 0.82	4.50 ± 1.04	t(55) = -4.54	<0.001**
ST, cognitive inhibition (time index)	26.59 ± 11.12	21.79 ± 8.77	t(52.9) = 1.81 ^a	0.07
GNG, motor inhibition (errors)	7.62 ± 4.87	5.64 ± 3.77	t(55) = -1.69	0.09
TOL, planification (accuracy)	5.5 ± 1.82	6.02 ± 1.0	t(55) = 1.10	0.10
RCST, shifting (perseveration errors)	1.90 ± 2.02	1.11 ± 1.34	t(48.8) = 1.74 ^a	0.09
AL, alertness (coefficient of variation)	0.30 ± 0.11	0.22 ± 0.06	t(44.8) = 3.16 ^a	0.003**

Values are presented as mean ± SD (standard deviation), except for sex, laterality, and pathological ADHD-RS score.

Abbreviations: DCD = Developmental Coordination Disorder; TD = Typically Developing children; Laterality = Edinburgh Handedness Inventory (Oldfield, 1971), R = right-handed, L = left-handed, A = ambidextrous; DCD-Q = The Developmental Coordination Disorder Questionnaire (Martini et al., 2011); ADHD-RS = Attentional Deficit Hyperactivity Disorder Rating Scale IV (DuPaul et al., 1998); MABC-2 = Movement Assessment Battery for Children, 2nd ed. (Henderson et al., 2007; Marquet-Doléac et al., 2016), percentile (pc) of the general scale and standard notes (SN) of the 3 subscales are reported; VCI = Verbal Comprehension Index of the Wechsler Intelligence Scale for Children, 5th ed. (WISC-V; Wechsler, 2016); VC = visual closure (DTVP-2; Hammill et al., 1993); BO = bars orientation recognition (Lacert, 1987); EH = eye-hand coordination (DTVP-2; Hammill et al., 1993); COPY = copying figures (DTVP-2; Hammill et al., 1993); BD = block design subtest (WISC-V; Wechsler, 2016); IHP = imitating hand positions (NEPSY-II; Korkman et al., 2007); MMS = manual motor sequences (NEPSY-II; Korkman et al., 2007); BTT = Corsi's block tapping test (Fournier and Albaret, 2013); STM = short-term memory; BDS = backward digit span (WISC-V; Wechsler, 2016); ST = non-reader Stroop test (Catale et al., 2014); GNG = Go-NoGo (Zimmermann and Fimm, 2004); TOL = tower of London (Shallice, 1982); RCST = revised Wisconsin Card Sorting Test (Nelson, 1976), AL = alertness test (Zimmermann and Fimm, 2004).

χ^2 = Chi-squared test; t = two-sample t test; ^a Welch t test, in cases of violation of homogeneity of variance. ^b Clinical test with outliers removed.

** $p < .002$ (0.05/22), statistical significance for clinical data (questionnaires, motor, and neuropsychological assessment) using Bonferroni correction for multiple comparison; * $p < .05$, uncorrected for clinical and demographic data.

state functional connectivity and spectral power in each frequency band. Of note, the same analyses performed without the covariates of no interest correlating with the group assignment (i.e., sex, verbal comprehension index and severity of the ADHD symptoms) did not reveal any significant differences between the groups (all $ps > .11$).

3.4. Relationship between resting-state functional connectivity, spectral power and behavioral measures

The outliers detected previously were removed from behavioral data before assessing the relationship between this specific behavioral data and spectral power or rsFC (n/10 subtests [range of n outliers]: DCD = 2/10 subtests [2–3]; TD = 2/10 subtests [1–3]). Only one subtest, copying figures (DTVP-2; Hammill et al., 1993), showed significant correlations with node power in the theta (threshold = 0.5077; $p = .0027$) and the high beta (threshold = 0.4499; $p = .0047$; all other $ps > .02$) bands and with rsFC in the alpha band (maximum statistics, threshold = 0.0082; $p = .003$; all other $ps > .02$). These results demonstrated that, in children with DCD, higher interhemispheric functional connectivity between sensorimotor areas (sensorimotor network, right frontal eye field and right pre-central sulcus) as well as higher power in right cerebellar lobule VIII was associated with lower performance in a visuomotor task. Fig. 5 and Table 3 detail these correlations.

4. Discussion

This MEG study revealed that children with DCD present atypical rsFC compared with their TD peers. Stronger rsFC was found in children with DCD mainly within the dorsal extrastriate network. The higher rsFC observed in children with DCD was not associated with the severity of motor symptoms nor with the visual perceptual/visuomotor impairments observed in a substantial proportion (65.5 %) of our DCD sample. However, a lower performance in one visuomotor task (copying figures) was associated with higher functional connectivity processes within the sensorimotor network and between the frontal eye field and the right precentral sulcus, and with a higher spectral power in the cerebellum (right lobule VIII).

The dorsal extrastriate network is known to be involved in sensorimotor transformations required for visually guided motor actions (Goodale and Milner, 1992; Milner and Goodale, 2008). The nodes involved in the atypical rsFC characterizing children with DCD play key roles in visuospatial processing/memory and attention shifts (i.e., bilateral precuneus; Cavanna and Trimble, 2006; Schott et al., 2019), in adaptation to environmental changes and to suboptimal consequences of previous actions (i.e., posterior cingulate cortex; Leech and Sharp, 2014; Pearson et al., 2011), in proprioception and stimulus-driven reorienting of attention (i.e., right supramarginal and angular gyri;

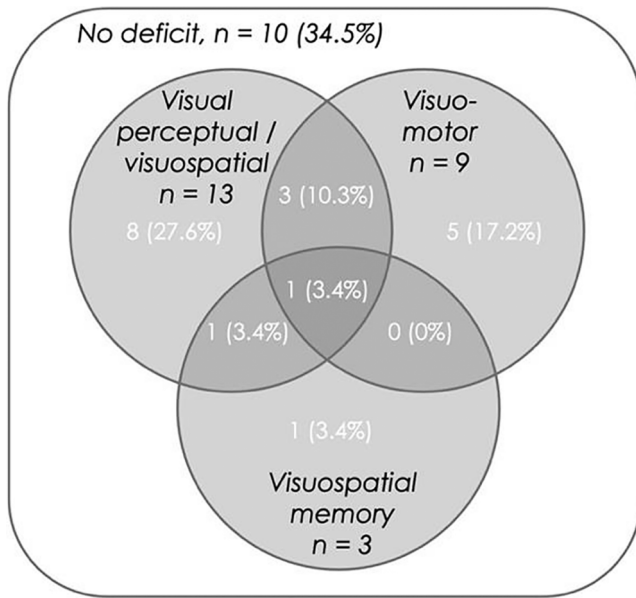


Fig. 3. Venn diagram of impairments in the DCD group for visual or visuospatial perception abilities (visual closure of the DTVP-2, Hammill et al., 1993; and bar orientation recognition, Lacert, 1987), visuomotor abilities (eye-hand coordination and copying of the DTVP-2, Hammill et al., 1993; and block design subtest of the WISC-V, Wechsler, 2016) and visuospatial short-term memory (Corsi's block tapping test, Fournier and Albaret, 2013). Individual results are compared to the normative data according to the age of the child. Impairment was considered if the child presented at least one score in the aforementioned abilities below the 5th percentile (or 1.65 standard deviation from the mean) of the normative data.

Ben-Shabat et al., 2015; Corbetta and Shulman, 2002, 2011), as well as in spatial cognition, semantic and multisensory integration (i.e., bilateral angular gyri; Price et al., 2016; Seghier, 2013). Furthermore, the

bilateral lobule V of the cerebellum is known to be involved in motor representations (Buckner, 2013; Guell et al., 2018). Some of these brain areas already exhibited lower functional connectivity with the sensorimotor network or altered activity in previous samples of children with DCD (precuneus, middle temporal gyrus, supramarginal gyrus, posterior cingulate cortex, and other subregions of the cerebellum, the crus I, lobules VI and IX; Debrabant et al., 2013; McLeod et al., 2014; Reynolds et al., 2015b; Reynolds et al., 2019; Rinat et al., 2020; Zwicker et al., 2010; Zwicker et al., 2011). These findings relate to the previous assumption that the functional brain architecture of children with DCD develops differently than their TD peers via the establishment of atypical neuronal and synaptic grouping within and between specific neural networks during brain maturation (Hadders-Algra, 2000; de Castelnau et al., 2008). This enhanced functional brain connectivity could reflect a characteristic brain trait of children with DCD compared to their TD peers. This hypothesis is supported by the absence of association with the classical measures of fine and gross motor activity (MABC-2; Henderson et al., 2007). Such atypical brain development (Chaudhury et al., 2016) might be driven by some genetic factors (Mosca et al., 2016) and lead to atypical motor behavior. It could also (and non-exclusively) be triggered by experience-dependent neural plasticity associated with an increased dependence on visuomotor processing during motor actions. Indeed, some findings suggest that children with DCD might rely more on sensory information to perform motor actions (Licari et al., 2015; Zwicker et al., 2010). Accordingly, as the enhanced functional brain connectivity was not related to the visual perceptual skills of the included children, it might be hypothesized that these children with DCD rely more on visual feedback and memory to guide their motor actions and try to compensate their motor impairments. Behavioral evidence already demonstrated that children with DCD are more dependent on vision and sensory feedback for motor control and balance than their TD peers (Bair et al., 2011; Wilson et al., 2013). These clinical observations led to hypothesize the existence of an internal modelling deficit in DCD (for a review, see Adams et al., 2014). Internal models enable, by the production of an efferent copy of the motor command, to predict the outcome of this command and to correct rapidly and online

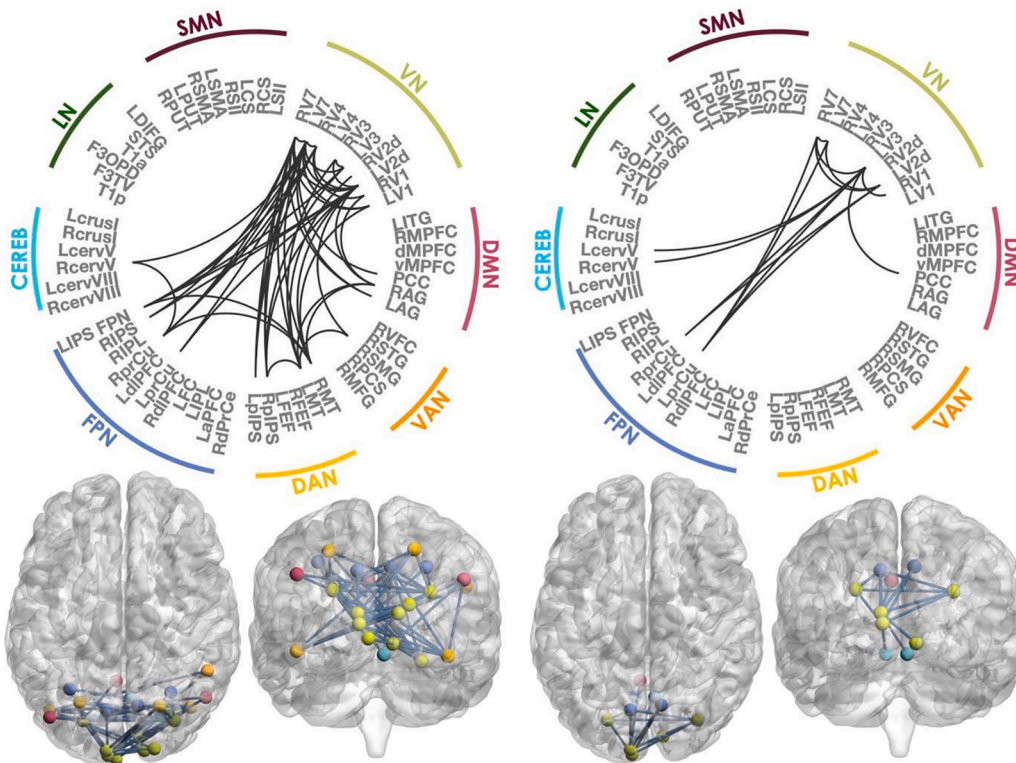


Fig. 4. Connections significantly stronger in children with DCD compared to TD peers in the alpha (Left) and the low beta (Right) bands. Brain is viewed from the above (Left) and back (Right). Brain figures were realized using the BrainNet viewer (Xia et al., 2013). Resting-state networks: LN = language network; SMN = sensorimotor network; VN = visual network; CEREB = cerebellar network; DMN = default mode network; FPN = frontoparietal network; DAN = dorsal attentional network; VAN = ventral attentional network.

Table 2
Differences in rsFC between DCD and TD children.

Alpha band (maxstat, $p = .00125$)					
Connections	29 DCD (mean \pm SD)	28 TD (mean \pm SD)	Connections	29 DCD (mean \pm SD)	28 TD (mean \pm SD)
RcervV - RprCu	0.097 \pm 0.057	0.078 \pm 0.050	RSMG - LV2d	0.053 \pm 0.046	0.029 \pm 0.024
RplPS - LMT	0.060 \pm 0.051	0.046 \pm 0.037	LV7 - RcervV	0.097 \pm 0.054	0.080 \pm 0.051
LMT - RAG	0.056 \pm 0.046	0.031 \pm 0.025	LV2d - LIPS _{FPN}	0.070 \pm 0.052	0.055 \pm 0.045
RMT - RAG	0.068 \pm 0.047	0.047 \pm 0.034	LV2d - RIPS	0.083 \pm 0.059	0.060 \pm 0.042
RMT - LIPS _{FPN}	0.062 \pm 0.046	0.043 \pm 0.041	LV2d - LprCu	0.110 \pm 0.067	0.095 \pm 0.065
RMT - RprCu	0.093 \pm 0.056	0.073 \pm 0.052	LV3 - LIPS _{FPN}	0.075 \pm 0.054	0.059 \pm 0.046
LMT - RSMG	0.047 \pm 0.036	0.022 \pm 0.021	RV4 - LIPS _{FPN}	0.070 \pm 0.047	0.050 \pm 0.045
LMT - RV2d	0.080 \pm 0.052	0.063 \pm 0.052	RV4 - LprCu	0.093 \pm 0.059	0.083 \pm 0.060
LMT - RV3	0.077 \pm 0.053	0.058 \pm 0.050	RV4 - RprCu	0.094 \pm 0.053	0.082 \pm 0.055
LMT - RV7	0.075 \pm 0.052	0.059 \pm 0.048	LV7 - LIPS _{FPN}	0.085 \pm 0.053	0.069 \pm 0.053
RMT - LV1	0.091 \pm 0.063	0.067 \pm 0.043	LV7 - RprCu	0.115 \pm 0.067	0.095 \pm 0.060
RMT - LV2d	0.103 \pm 0.068	0.074 \pm 0.042	RV7 - RIPS	0.101 \pm 0.055	0.074 \pm 0.049
RMT - LV7	0.087 \pm 0.058	0.067 \pm 0.049	RV7 - RprCu	0.118 \pm 0.060	0.097 \pm 0.062
LpIPS - LV7	0.090 \pm 0.060	0.072 \pm 0.052	LV1 - LV7	0.093 \pm 0.058	0.075 \pm 0.058
LpIPS - RV4	0.070 \pm 0.049	0.053 \pm 0.046	LV1 - RV7	0.098 \pm 0.061	0.078 \pm 0.053
LpIPS - RV7	0.084 \pm 0.055	0.071 \pm 0.055	LV2d - RV3	0.112 \pm 0.069	0.091 \pm 0.058
RpIPS - LV2d	0.086 \pm 0.059	0.064 \pm 0.041	LV2d - RV4	0.114 \pm 0.068	0.088 \pm 0.053
RpIPS - LV3	0.089 \pm 0.063	0.070 \pm 0.043	LV2d - LV7	0.107 \pm 0.064	0.082 \pm 0.062
RpIPS - LV7	0.094 \pm 0.065	0.076 \pm 0.051	LV2d - RV7	0.111 \pm 0.071	0.085 \pm 0.055
RpIPS - RV7	0.103 \pm 0.057	0.079 \pm 0.050	LV3 - RV3	0.113 \pm 0.070	0.096 \pm 0.061
PCC - LV7	0.105 \pm 0.062	0.091 \pm 0.065	LV3 - LV7	0.104 \pm 0.068	0.089 \pm 0.063
LAG - LV7	0.071 \pm 0.063	0.056 \pm 0.042	RV1 - RV4	0.119 \pm 0.067	0.095 \pm 0.060
LAG - RV7	0.068 \pm 0.053	0.053 \pm 0.045	RV4 - LV7	0.094 \pm 0.052	0.079 \pm 0.054
RAG - LV2d	0.064 \pm 0.057	0.043 \pm 0.034	LV7 - RV7	0.112 \pm 0.065	0.090 \pm 0.064
RAG - RV1	0.070 \pm 0.054	0.050 \pm 0.041			

Low beta band (maxtstat, $p = .00025$)					
Connections	29 DCD (mean \pm SD)	28 TD (mean \pm SD)	Connections	29 DCD (mean \pm SD)	28 TD (mean \pm SD)
PCC - LV3	0.100 \pm 0.057	0.094 \pm 0.061	LV7 - LprCu	0.111 \pm 0.069	0.102 \pm 0.070
LV3 - RcervV	0.098 \pm 0.058	0.090 \pm 0.051	RV7 - LprCu	0.116 \pm 0.063	0.100 \pm 0.069
LV3 - LcervV	0.096 \pm 0.059	0.086 \pm 0.051	RV1 - LV3	0.116 \pm 0.064	0.103 \pm 0.059
LV2d - LprCu	0.110 \pm 0.067	0.095 \pm 0.065	LV2d - LV7	0.107 \pm 0.064	0.082 \pm 0.062
LV2d - RprCu	0.107 \pm 0.060	0.088 \pm 0.056	LV2d - RV7	0.111 \pm 0.071	0.085 \pm 0.055
LV3 - LprCu	0.109 \pm 0.065	0.101 \pm 0.070	LV3 - RV7	0.114 \pm 0.072	0.093 \pm 0.064
LV3 - RprCu	0.110 \pm 0.063	0.096 \pm 0.060	LV7 - RV7	0.112 \pm 0.065	0.090 \pm 0.064

RSNs = resting-state networks; L/R = left / right hemisphere; CEREB = cerebellar network; DAN = dorsal attentional network; DMN = default mode network; FPN = frontoparietal network; VAN = ventral attentional network; VN = visual network.

the ongoing movement, before the neural availability of the sensory feedback (Wolpert and Flanagan, 2001). In regards of this hypothesis, children with DCD present impairments on several aspects of movement prediction (Adams et al., 2017), online adjustment and movement control (Fuelscher et al., 2015), and mental manipulation of their body schema (Reynolds et al., 2015b). An actual deficit in the mental representation of the movements could lead children with DCD to rely more on sensory (and especially visual) feedback and therefore to develop stronger rsFC between the brain areas involved in action-oriented visual function (Hutchison and Gallivan, 2018; Rizzolatti and Matelli, 2003), adjustment to environment and feedback (Leech and Sharp, 2014; Pearson et al., 2011), visuospatial (Cavanna and Trimble, 2006; Schott et al., 2019) and semantic memory (Price et al., 2016). Still, based on the available data, the pathophysiological mechanisms at the basis of the observed increase in rsFC is rather undetermined. Future studies should adopt longitudinal investigations in children with DCD to explore the development of this atypical functional brain architecture. Performing a task specifically assessing the internal modelling (e.g., overt and covert movements; for a review, see Adams et al., 2014) during MEG recording might also bring new evidence in favor of this hypothesis. Indeed, this work was designed to characterize the “intrinsic” (i.e., context invariant; Engel et al., 2013) functional brain architecture of children with DCD using a resting-state experimental paradigm. Investigating “extrinsic” (i.e., task-dependent) functional brain connectivity while children with DCD perform motor, perceptual or cognitive tasks might help to better characterize the differences in functional brain architecture of children

with DCD compared with their TD peers.

Beside those changes in rsFC, correlation analyses revealed that, in children with DCD, lower visuomotor performance was associated with (i) a stronger rsFC between sensorimotor brain regions, and (ii) a higher spectral power (theta and high beta) within subsections of the cerebellum involved in motor representation (right lobule VIII; Buckner, 2013; Guell et al., 2018). Previous evidence demonstrated that children with DCD exhibiting higher intra-individual variability in unimanual motor coordination (while producing a motor response synchronous to a visual stimulus) also presented enhanced intrahemispheric brain functional connectivity (based on EEG coherence; de Castelnau et al., 2008). Surprisingly, in our sample, children with DCD and with a low performance in a unimanual visuomotor task (i.e., copying figures; Hammill et al., 1993) also presented higher interhemispheric rsFC between sensorimotor brain regions. This might reflect an abnormal hemispheric brain specialization possibly playing a key role in the DCD pathophysiology (Querne et al., 2008). Interestingly, the above-mentioned copying figures task (Hammill et al., 1993) was the only one in which none of the children with DCD presented any impairment compared with the normative data. It has been suggested that brain compensatory mechanisms with a wider recruitment of brain regions and greater engagement of cortical resources might be at play to enable children with DCD to reach similar performance compared with TD peers or other neurodevelopmental disorder in various motor or executive tasks (Biotteau et al., 2017; Koch et al., 2018; Pangelinan et al., 2013; Zwicker et al., 2010). Our correlational findings might therefore suggest that children

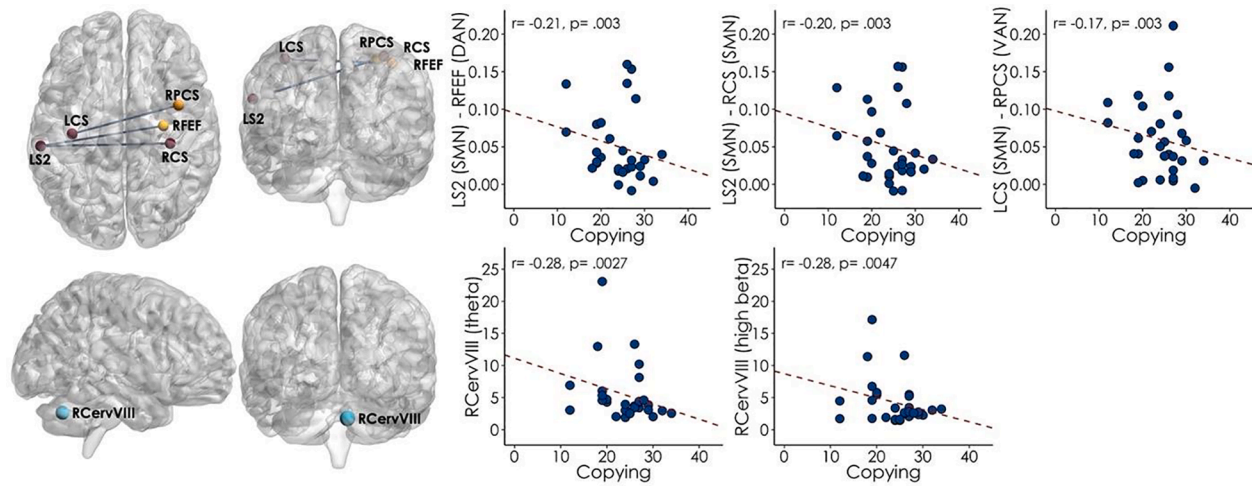


Fig. 5. Significant correlations between performance in copying figures (higher scores represent higher number of figures correctly achieved) and rsFC in the alpha band (**Top**) and power in the theta and the high beta bands (**Bottom**). **Left.** Connections or nodes negatively correlating with performance in copying figures, represented on the MNI brain (viewed from the top for rsFC and right side for power (Left) or the back (Right)). These plots were realized using the BrainNet viewer (Xia et al., 2013). **Right.** Scatter plots for each significant correlation. L/R = left/right hemisphere, SMN = sensorimotor network; DAN = dorsal attentional network; VAN = ventral attentional network; LS2 = Left Second Somatosensory; RFEF = Right Frontal Eye Field; RCS = Right Central Sulcus; RPCS = Right Pre-Central Sulcus; RCervVIII = right lobule VIII of the cerebellum.

Table 3

Significant correlations between whole brain rsFC, power and copying score in children with developmental coordination disorder.

Connection / node	Corresponding RSNs	Frequency band	Maxstat p-value	R	t-value
Resting state functional connectivity					
LS2 - RFEF	SMN - DAN	Alpha	0.003	-0.21	-3.214
LS2 - RCS	SMN - SMN			-0.20	-3.336
LCS - RPCS	SMN - VAN			-0.17	-2.599
Spectral power					
RcervVIII	CEREB	Theta	0.0027	-0.28	-2.131
RcervVIII	CEREB	High beta	0.0047	-0.28	-2.206

L/R = left/right hemisphere; RSNs = resting state networks; SMN = sensorimotor network; DAN = dorsal attentional network; VAN = ventral attentional network; CEREB = cerebellar network.

with the lowest visuomotor performance needed higher interhemispheric functional connectivity between some nodes of the sensorimotor network to reach a performance within the normative range.

This study contributes to the small but growing literature showing evidence of atypical brain functioning in children with DCD (for reviews, see Biotteau et al., 2016; Fuelscher et al., 2018; Hyde et al., 2019). The observed enhancement in functional brain connectivity within the dorsal extrastriate visual brain system and the absence of association with visual perceptual or motor impairments call for further investigations of the potential compensatory processes at play in DCD. Visual networks were excluded from previous resting-state fMRI investigation due to the inability to control for eye behavior and arousal during fMRI recordings (Rinat et al., 2020). This study highlights that electrophysiological methods such as MEG can provide good alternative to study the visual networks in children with DCD as behavior can be controlled during (i.e., video monitoring) and after (i.e., comparison of quantity of eye blinks and alpha power) the recordings.

A first limitation of this study is that our DCD sample was composed of children with and without concurrent ADHD. We controlled for the severity of ADHD symptoms using the parental questionnaire ADHD-RS-IV as covariate of no-interest. The use of a questionnaire represents a limitation as it only reflects the clinical severity of the observable symptoms. It would be of interest to compare large samples of children with DCD only to children with concurrent ADHD to better understand

the brain alterations that are specific to DCD and the differences with children presenting associated disorders. We introduced several possible confounding factors (i.e., sex, age, the severity of the ADHD symptoms, the verbal comprehension index and laterality) as covariates of no interest in the group comparison analysis. Some of these covariates (sex, severity of ADHD symptoms, verbal comprehension index) did correlate with the group assignment, which might have affected the sensitivity of our group comparison analysis. Still, removing these covariates for the analysis did not reveal any significant results, which is explained by the fact that including confounding variables in regression models might enable to control for irrelevant variance and therefore increase the statistical power (Watson et al., 2013). Second, the sample size of the groups of children did not enable us to cross-validate our results. As to the best of our knowledge, no previous study investigated rsFC in children with DCD compared to TD peers using MEG, we cannot confront our results to previous findings. These results should then be replicated either with MEG as in this study, or with fMRI while including the visual network and controlling for eye behavior through eye tracking devices. The recruitment of larger groups of children with DCD and TD children would allow to validate the results obtained on the first half of the children on the second half of the participants; providing that both group of children with DCD are matched in terms of motor and visuomotor impairments as well as comorbidities. Third, we used an *a priori* approach to investigate the functional brain architecture as we limited our investigation to 59 nodes of interest. Differences might nevertheless also occur in other parts of the brain. This approach offers however the advantages to comprise multiple seeds corresponding to the key regions of the main functional networks and to study the correlations within and across networks (Della Penna et al., 2019; de Pasquale et al., 2012). The spatial topography of these networks, named after their putative function, was first unraveled in task and consistently reproduced at rest. However, in the context of this study, the brain regions showing differential rsFC between groups were not interpreted in terms of these RSNs as the nodes involved were mostly interpreted as belonging to the visual system. Despite the classification into a limited number of major brain resting state networks, some nodes may be involved in several brain networks (e.g., Sjøgård et al., 2021), possibly limiting the interpretations in terms of cross-networks interactions. Fourth, as children participated in a rather long experimental protocol, we chose to divide the protocol in several sessions. The number of sessions varied among participants to respect the fatigue level of some individual participants

and to ensure that they would realize the entire protocol. Finally, although debated, MEG is considered to be less sensitive to deep brain sources (Hillebrand and Barnes, 2002), especially in children given their small head size (Gaetz et al., 2008; Pang et al., 2003). This might therefore limit the ability to unravel abnormalities in brain structures considered to be involved in DCD pathophysiology such as the basal ganglia (Bo and Lee, 2013; Querne et al., 2008; McLeod et al., 2014; Reynolds et al., 2019; Zwicker et al., 2009).

5. Conclusion

This MEG study showed that children with DCD present atypical functional brain architecture mainly within the dorsal extrastriate network compared to their TD peers. The observed enhancement in functional brain connectivity in children with DCD did not correlate with their motor nor visual perceptual abilities. This pattern of functional brain architecture might therefore correspond to a genetically-determined characteristic brain trait of children with DCD or to experienced-dependent neural plasticity associated with an increased reliance on visual feedback to compensate for motor or movement representation deficit, independently of motor performance. Altogether, this study brings unprecedented behavioral and electrophysiological evidence showing, once again, that DCD is not just a motor disorder.

6. Data statement

The behavioral data and raw neuroimaging data that support the findings of this study are available upon request from the corresponding author and after acceptance by institutional authorities (CUB Hôpital Erasme and Université libre de Bruxelles). The data are not publicly available due to ethical restrictions. Anonymized functional connectivity matrices and the statistical analysis script are available upon request from the corresponding author.

CRedit authorship contribution statement

Dorine Van Dyck: Conceptualization, Methodology, Investigation, Formal analysis, Writing – original draft, Writing – review & editing. **Nicolas Deconinck:** Conceptualization, Resources, Project administration, Writing – review & editing, Funding acquisition. **Alec Aeby:** Conceptualization, Resources, Writing – review & editing, Funding acquisition. **Simon Bajot:** Conceptualization, Resources, Writing – review & editing, Funding acquisition. **Nicolas Coquelet:** Software, Writing – review & editing. **Nicola Trotta:** Resources, Writing – review & editing. **Antonin Rovai:** Resources, Writing – review & editing. **Serge Goldman:** Resources, Writing – review & editing. **Charline Urbain:** Resources, Writing – review & editing. **Vincent Wens:** Methodology, Software, Formal analysis, Writing – original draft, Writing – review & editing. **Xavier De Tiège:** Conceptualization, Methodology, Resources, Formal analysis, Project administration, Writing – original draft, Writing – review & editing, Funding acquisition.

Declaration of Competing Interest

The authors declare that they have no known competing financial interests or personal relationships that could have appeared to influence the work reported in this paper.

Acknowledgements

Dorine Van Dyck was supported by “The Belgian Kids’ Fund for Pediatric Research” (Brussels, Belgium; <https://www.belgiankidsfund.be/fr/index.cfm>) and is supported by the “Fondation ROGER DE SPOELBERCH” (Geneva, Switzerland; <https://www.fondation-roger-despoelberch.ch/>). Xavier De Tiège is Clinical Researcher at the Fonds de la Recherche Scientifique (FRS-FNRS, Brussels, Belgium).

The MEG project at the CUB Hôpital Erasme is financially supported by the Fonds Erasme (Research Convention, Brussels, Belgium; <https://www.fondserasme.org/fonds-erasme-pour-la-recherche-medicale>). The PET-MRI project at the CUB Hôpital Erasme is financially supported by the Association Vinçotte Nuclear (AVN, Brussels, Belgium).

The authors would like to warmly thank all the children and their parents for their participation as well as the neuropediatricians and health professionals for their involvement and help to recruit participants: Dr Fanny Badin (CHU Tivoli), Mrs Marie Champeix (HUDERF), Dr Sophie Galer (HUDERF), Dr Sophie Ghariani (UCL Saint-Luc and Centre La Manivelle), Dr Elodie Juvené (HUDERF), Dr Despoina Mandelenaki (HUDERF), Dr Cynthia Prigogine (HUDERF), Dr Claudine Sculier (CUB Hôpital Erasme), Dr Tayeb Sekhara (Clinique Ste-Anne St-Remi, CHIREC), and Dr Audrey Van Hecke (HUDERF and CHU Saint-Pierre).

Appendix A. Supplementary data

Supplementary data to this article can be found online at <https://doi.org/10.1016/j.nicl.2021.102928>.

References

- Adams, I.L.J., Lust, J.M., Wilson, P.H., Steenbergen, B., 2014. Compromised motor control in children with DCD: A deficit in the internal model?—a systematic review. *Neurosci. Biobehav. Rev.* 47, 225–244. <https://doi.org/10.1016/j.neubiorev.2014.08.011>.
- Adams, I.L.J., Lust, J.M., Wilson, P.H., Steenbergen, B., 2017. Testing predictive control of movement in children with developmental coordination disorder using converging operations. *Br. J. Psychol.* 108 (1), 73–90. <https://doi.org/10.1111/bjop.12183>.
- Alloway, T.P., Rajendran, G., Archibald, L.M.D., 2009. Working Memory in Children With Developmental Disorders. *J. Learn. Disab.* 42 (4), 372–382. <https://doi.org/10.1177/0022219409335214>.
- American Psychiatric Association, Ed., 2013. Diagnostic and statistical manual of mental disorders: DSM-5, 5th ed. American Psychiatric Publishing.
- Ashburner, J., Friston, K.J., 1999. Nonlinear spatial normalization using basis functions. *Hum. Brain Mapp.* 7 (4), 254–266.
- Bair, W.-N., Barela, J.A., Whitall, J., Jeka, J.J., Clark, J.E., 2011. Children with Developmental Coordination Disorder benefit from using vision in combination with touch information for quiet standing. *Gait Posture* 34 (2), 183–190. <https://doi.org/10.1016/j.gaitpost.2011.04.007>.
- Barry, R.J., Clarke, A.R., Johnstone, S.J., Magee, C.A., Rushby, J.A., 2007. EEG differences between eyes-closed and eyes-open resting conditions. *Clin. Neurophysiol.* 118 (12), 2765–2773. <https://doi.org/10.1016/j.clinph.2007.07.028>.
- Ben-Shabat, E., Matyas, T.A., Pell, G.S., Brodtmann, A., Carey, L.M., 2015. The Right Supramarginal Gyrus Is Important for Proprioception in Healthy and Stroke-Affected Participants: A Functional MRI Study. *Front. Neurol.* 6, 248. <https://doi.org/10.3389/fneur.2015.00248>.
- Bernardi, M., Leonard, H.C., Hill, E.L., Botting, N., Henry, L.A., 2018. Executive functions in children with developmental coordination disorder: A 2-year follow-up study. *Dev. Med. Child Neurol.* 60 (3), 306–313. <https://doi.org/10.1111/dmcn.13640>.
- Biotteau, M., Chaix, Y., Blais, M., Tallet, J., Péran, P., Albaret, J.-M., 2016. Neural Signature of DCD: A Critical Review of MRI Neuroimaging Studies. *Front. Neurol.* 7 <https://doi.org/10.3389/fneur.2016.00227>.
- Biotteau, M., Péran, P., Vayssière, N., Tallet, J., Albaret, J.-M., Chaix, Y., 2017. Neural changes associated to procedural learning and automatization process in Developmental Coordination Disorder and/or Developmental Dyslexia. *Eur. J. Paediatr. Neurol.* 21 (2), 286–299. <https://doi.org/10.1016/j.ejpn.2016.07.025>.
- Blais, M., Amantini, D., Albaret, J.-M., Chaix, Y., Tallet, J., 2018. Atypical inter-hemispheric communication correlates with altered motor inhibition during learning of a new bimanual coordination pattern in developmental coordination disorder. *Dev. Sci.* 21 (3), e12563. <https://doi.org/10.1111/desc.2018.21.issue-310.1111/desc.12563>.
- Bo, J., Lee, C.-M., 2013. Motor skill learning in children with Developmental Coordination Disorder. *Res. Dev. Disabil.* 34 (6), 2047–2055. <https://doi.org/10.1016/j.ridd.2013.03.012>.
- Brookes, M.J., Woolrich, M., Luchoo, H., Price, D., Hale, J.R., Stephenson, M.C., Barnes, G.R., Smith, S.M., Morris, P.G., 2011. Investigating the electrophysiological basis of resting state networks using magnetoencephalography. *Proc. Natl. Acad. Sci.* 108 (40), 16783–16788. <https://doi.org/10.1073/pnas.1112685108>.
- Brookes, M.J., Woolrich, M.W., Barnes, G.R., 2012. Measuring functional connectivity in MEG: A multivariate approach insensitive to linear source leakage. *NeuroImage* 63 (2), 910–920. <https://doi.org/10.1016/j.neuroimage.2012.03.048>.
- Buckner, R.L., 2013. The Cerebellum and Cognitive Function: 25 Years of Insight from Anatomy and Neuroimaging. *Neuron* 80 (3), 807–815. <https://doi.org/10.1016/j.neuron.2013.10.044>.
- Catale, C., Lejeune, C., Schmitz, X., Meulemans, T., 2014. Validation d’un test d’inhibition auprès d’enfants présentant un trouble déficitaire de l’attention avec ou

- sans hyperactivité. *Canad. J. Behav. Sci. / Revue canadienne des sciences du comportement* 46 (1), 66–72. <https://doi.org/10.1037/a0031006>.
- Cavanna, A.E., Trimble, M.R., 2006. The precuneus: A review of its functional anatomy and behavioural correlates. *Brain* 129 (3), 564–583. <https://doi.org/10.1093/brain/awl004>.
- Chaudhury, S., Sharma, V., Kumar, V., Nag, T.C., Wadhwa, S., 2016. Activity-dependent synaptic plasticity modulates the critical phase of brain development. *Brain Dev.* 38 (4), 355–363. <https://doi.org/10.1016/j.braindev.2015.10.008>.
- Cheng, C.-H., Ju, Y.-Y., Chang, H.-W., Chen, C.-L., Pei, Y.-C., Tseng, K.C., Cheng, H.-Y.-K., 2014. Motor impairments screened by the Movement Assessment Battery for Children-2 are related to the visual-perceptual deficits in children with Developmental Coordination Disorder. *Res. Dev. Disabil.* 35 (9), 2172–2179. <https://doi.org/10.1016/j.ridd.2014.05.009>.
- Cignetti, F., Nemmi, F., Vaugoyeau, M., Girard, N., Albaret, J., Chaix, Y., Péran, P., Assaïante, C., 2020. Intrinsic Cortico-Subcortical Functional Connectivity in Developmental Dyslexia and Developmental Coordination Disorder. *Cerebr. Cortex Commun.* 1 (1), 1–14. <https://doi.org/10.1093/texcom/tgaa011>.
- Coquelet, N., De Tiège, X., Destoko, F., Roshchupkina, L., Bourguignon, M., Goldman, S., Peigneux, P., Wens, V., 2020. Comparing MEG and high-density EEG for intrinsic functional connectivity mapping. *NeuroImage* 210, 116556. <https://doi.org/10.1016/j.neuroimage.2020.116556>.
- Corbetta, M., Shulman, G.L., 2002. Control of goal-directed and stimulus-driven attention in the brain. *Nat. Rev. Neurosci.* 3 (3), 201–215. <https://doi.org/10.1038/nrn755>.
- Corbetta, M., Shulman, G.L., 2011. Spatial neglect and attention networks. *Annu. Rev. Neurosci.* 34 (1), 569–599. <https://doi.org/10.1146/annurev-neuro-061010-113731>.
- Dale, A.M., Sereno, M.I., 1993. Improved Localization of Cortical Activity by Combining EEG and MEG with MRI Cortical Surface Reconstruction: A Linear Approach. *J. Cognit. Neurosci.* 5 (2), 162–176. <https://doi.org/10.1162/jocn.1993.5.2.162>.
- de Castelneau, P., Albaret, J.-M., Chaix, Y., Zanone, P.-G., 2008. A study of EEG coherence in DCD children during motor synchronization task. *Hum. Mov. Sci.* 27 (2), 230–241. <https://doi.org/10.1016/j.humov.2008.02.006>.
- de Pasquale, F., Della Penna, S., Snyder, A.Z., Lewis, C., Mantini, D., Marzetti, L., Belardinelli, P., Ciancetta, L., Pizzella, V., Romani, G.L., Corbetta, M., 2010. Temporal dynamics of spontaneous MEG activity in brain networks. *Proc. Natl. Acad. Sci.* 107 (13), 6040–6045. <https://doi.org/10.1073/pnas.0913863107>.
- de Pasquale, F., Della Penna, S., Snyder, A.Z., Marzetti, L., Pizzella, V., Romani, G.L., Corbetta, M., 2012. A Cortical Core for Dynamic Integration of Functional Networks in the Resting Human Brain. *Neuron* 74 (4), 753–764. <https://doi.org/10.1016/j.neuron.2012.03.031>.
- De Tiège, X., Op de Beeck, M., Funke, M., Legros, B., Parkkonen, L., Goldman, S., Van Boegaert, P., 2008. Recording epileptic activity with MEG in a light-weight magnetic shield. *Epilepsy Res.* 82 (2–3), 227–231. <https://doi.org/10.1016/j.eplepsyres.2008.08.011>.
- Debrabant, J., Gheysen, F., Caeyenberghs, K., Van Waelvelde, H., Vingerhoets, G., 2013. Neural underpinnings of impaired predictive motor timing in children with Developmental Coordination Disorder. *Res. Dev. Disabil.* 34 (5), 1478–1487. <https://doi.org/10.1016/j.ridd.2013.02.008>.
- Deco, G., Corbetta, M., 2011. The Dynamical Balance of the Brain at Rest. *Neuroscientist* 17 (1), 107–123. <https://doi.org/10.1177/1073858409354384>.
- Della Penna, S., Corbetta, M., Wens, V., de Pasquale, F., 2019. The Impact of the Geometric Correction Scheme on MEG Functional Topology at Rest. *Front. Neurosci.* 13, 1114. <https://doi.org/10.3389/fnins.2019.01114>.
- Dewey, D., 2018. What Is Comorbidity and Why Does It Matter in Neurodevelopmental Disorders? *Curr. Dev. Disord. Rep.* 5 (4), 235–242. <https://doi.org/10.1007/s40474-018-0152-3>.
- Dewey, D., Kaplan, B.J., Crawford, S.G., Wilson, B.N., 2002. Developmental coordination disorder: Associated problems in attention, learning, and psychosocial adjustment. *Hum. Mov. Sci.* 21 (5–6), 905–918. [https://doi.org/10.1016/S0167-9457\(02\)00163-X](https://doi.org/10.1016/S0167-9457(02)00163-X).
- DuPaul, G., Power, T., Anastopoulos, A., Reid, R., 1998. *ADHD Rating Scale—IV: Checklists, norms, and clinical interpretation*. Guilford Press.
- Engel, A.K., Gerloff, C., Hiltgetag, C.C., Nolte, G., 2013. Intrinsic Coupling Modes: Multiscale Interactions in Ongoing Brain Activity. *Neuron* 80 (4), 867–886. <https://doi.org/10.1016/j.neuron.2013.09.038>.
- Fischl, B., 2012. FreeSurfer. *NeuroImage* 62 (2), 774–781. <https://doi.org/10.1016/j.neuroimage.2012.01.021>.
- Fournier, M., Albaret, J.-M., 2013. Étalonnage des blocs de Corsi sur une population d'enfants scolarisés du CP à la 6e. *Développements* 16–17 (3), 76. <https://doi.org/10.3917/devel.016.0076>.
- Fox, M.D., Raichle, M.E., 2007. Spontaneous fluctuations in brain activity observed with functional magnetic resonance imaging. *Nat. Rev. Neurosci.* 8 (9), 700–711. <https://doi.org/10.1038/nrn2201>.
- Fuelscher, I., Caeyenberghs, K., Enticott, P.G., Williams, J., Lum, J., Hyde, C., 2018. Differential activation of brain areas in children with developmental coordination disorder during tasks of manual dexterity: An ALE meta-analysis. *Neurosci. Biobehav. Rev.* 86, 77–84. <https://doi.org/10.1016/j.neubiorev.2018.01.002>.
- Fuelscher, I., Williams, J., Enticott, P.G., Hyde, C., 2015. Reduced motor imagery efficiency is associated with online control difficulties in children with probable developmental coordination disorder. *Res. Dev. Disabil.* 45–46, 239–252. <https://doi.org/10.1016/j.ridd.2015.07.027>.
- Gaetz, W., Otsubo, H., Pang, E.W., 2008. Magnetoencephalography for clinical pediatrics: The effect of head positioning on measurement of somatosensory-evoked fields. *Clin. Neurophysiol.* 119 (8), 1923–1933. <https://doi.org/10.1016/j.clinph.2008.04.291>.
- Geuze, R.H., 2005. Postural Control in Children With Developmental Coordination Disorder. *Neural Plasticity* 12 (2–3), 183–196. <https://doi.org/10.1155/NP.2005.183>.
- Godfrey, O., Gibbons, L., Diouf, M., Nyenhuis, D., Roussel, M., Black, S., Bugnicourt, J. M., 2014. Validation of an integrated method for determining cognitive ability: Implications for routine assessments and clinical trials. *Cortex* 54, 51–62. <https://doi.org/10.1016/j.cortex.2014.01.016>.
- Goodale, M.A., Milner, A.D., 1992. Separate visual pathways for perception and action. *Trends Neurosci.* 15 (1), 20–25. [https://doi.org/10.1016/0166-2236\(92\)90344-8](https://doi.org/10.1016/0166-2236(92)90344-8).
- Gramfort, A., Luessi, M., Larson, E., Engemann, D.A., Strohmeier, D., Brodbeck, C., Parkkonen, L., Hämäläinen, M.S., 2014. MNE software for processing MEG and EEG data. *NeuroImage* 86, 446–460. <https://doi.org/10.1016/j.neuroimage.2013.10.027>.
- Guell, X., Schmahmann, J.D., Gabrieli, J.D.E., Ghosh, S.S., 2018. Functional gradients of the cerebellum. *ELife* 7. <https://doi.org/10.7554/eLife.36652>.
- Hadders-Algra, M., 2000. The neuronal group selection theory: Promising principles for understanding and treating developmental motor disorders. *Dev. Med. Child Neurol.* 42 (10), 707–715. <https://doi.org/10.1111/j.1469-8749.2000.tb00687.x>.
- Hammill, D.D., Pearson, N.A., Vores, J.K., 1993. *Developmental Test of Visual Perception, 2nd ed.* Pro-ed.
- Henderson, S., Sugden, D., Barnett, A.L., 2007. Movement assessment battery for children-2 (MABC-2) (Pearson Clinical).
- Hillebrand, A., Barnes, G.R., 2002. A Quantitative Assessment of the Sensitivity of Whole-Head MEG to Activity in the Adult Human Cortex. *NeuroImage* 16 (3), 638–650. <https://doi.org/10.1006/nimg.2002.1102>.
- Hipp, J.F., Hawellek, D.J., Corbetta, M., Siegel, M., Engel, A.K., 2012. Large-scale cortical correlation structure of spontaneous oscillatory activity. *Nat. Neurosci.* 15 (6), 884–890. <https://doi.org/10.1038/nn.3101>.
- Hoare, D., 1994. Subtypes of Developmental Coordination Disorder. *Adapted Phys. Activity Quart.* 11 (2), 158–169. <https://doi.org/10.1123/apaq.11.2.158>.
- Hutchison, R.M., Gallivan, J.P., 2018. Functional coupling between frontoparietal and occipitotemporal pathways during action and perception. *Cortex* 98, 8–27. <https://doi.org/10.1016/j.cortex.2016.10.020>.
- Hyde, C., Fuelscher, I., Williams, J., 2019. Neurophysiological Approaches to Understanding Motor Control in DCD: Current Trends and Future Directions. *Curr. Dev. Disord. Rep.* 6 (2), 78–86. <https://doi.org/10.1007/s40474-019-00161-1>.
- Kadesjö, B., Gillberg, C., 1998. Attention deficits and clumsiness in Swedish 7-year-old children. *Dev. Med. Child Neurol.* 40 (12), 796–804. <https://doi.org/10.1111/j.1469-8749.1998.tb12356.x>.
- Koch, J.K.L., Miguel, H., Smiley-Oyen, A.L., 2018. Prefrontal activation during Stroop and Wisconsin card sort tasks in children with developmental coordination disorder: A NIRS study. *Exp. Brain Res.* 236 (11), 3053–3064. <https://doi.org/10.1007/s00221-018-5358-4>.
- Korkman, M., Kemp, S., Kirk, U., 2007. NEPSY-II. Pearson.
- Lacert, P., 1987. *Test de repérage topologique et directionnel*. EAP.
- Largo, R.H., Pfister, D., Molinari, L., Kundu, S., Lipp, A., Due, G., 1989. Significance of prenatal, perinatal and postnatal factors in the development of AGA preterm infants at five to seven years 31 (4), 440–456.
- Leech, R., Sharp, D.J., 2014. The role of the posterior cingulate cortex in cognition and disease. *Brain* 137 (1), 12–32. <https://doi.org/10.1093/brain/awt162>.
- Leonard, H.C., Bernardi, M., Hill, E.L., Henry, L.A., 2015. Executive Functioning, Motor Difficulties, and Developmental Coordination Disorder. *Dev. Neuropsychol.* 40 (4), 201–215. <https://doi.org/10.1080/87565641.2014.997933>.
- Leys, C., Ley, C., Klein, O., Bernard, P., Licata, L., 2013. Detecting outliers: Do not use standard deviation around the mean, use absolute deviation around the median. *J. Exp. Soc. Psychol.* 49 (4), 764–766. <https://doi.org/10.1016/j.jesp.2013.03.013>.
- Licari, M.K., Billington, J., Reid, S.L., Wann, J.P., Elliott, C.M., Winsor, A.M., Robins, E., Thornton, A.L., Jones, R., Bynevelt, M., 2015. Cortical functioning in children with developmental coordination disorder: A motor overflow study. *Exp. Brain Res.* 233 (6), 1703–1710. <https://doi.org/10.1007/s00221-015-4243-7>.
- Liu, Q., Farahibozorg, S., Porcaro, C., Wenderoth, N., Mantini, D., 2017. Detecting large-scale networks in the human brain using high-density electroencephalography: Imaging Brain Networks with High Density EEG. *Hum. Brain Mapp.* 38 (9), 4631–4643. <https://doi.org/10.1002/hbm.23688>.
- Liu, Q., Ganzetti, M., Wenderoth, N., Mantini, D., 2018. Detecting Large-Scale Brain Networks Using EEG: Impact of Electrode Density, Head Modeling and Source Localization. *Front. Neuroinf.* 12. <https://doi.org/10.3389/fninf.2018.00004>.
- Liuzzi, L., Gascoyne, L.E., Tewarie, P.K., Barratt, E.L., Boto, E., Brookes, M.J., 2017. Optimising experimental design for MEG resting state functional connectivity measurement. *NeuroImage* 155, 565–576. <https://doi.org/10.1016/j.neuroimage.2016.11.064>.
- Marquet-Dolac, J., Soppelsa, R., Albaret, J.-M., 2016. *Batterie d'évaluation du mouvement chez l'enfant-seconde édition (MABC-2). Adaptation française, ECPA par Pearson*.
- Martini, R., St-Pierre, M.-F., Wilson, B.N., 2011. French Canadian Cross-Cultural Adaptation of the Developmental Coordination Disorder Questionnaire '07: DCDQ-FC. *Can. J. Occup. Ther.* 78 (5), 318–327. <https://doi.org/10.2182/cjot.2011.78.5.7>.
- McLeod, K.R., Langevin, L.M., Dewey, D., Goodyear, B.G., 2016. Atypical within- and between-hemisphere motor network functional connections in children with developmental coordination disorder and attention-deficit/hyperactivity disorder. *NeuroImage: Clin.* 12, 157–164. <https://doi.org/10.1016/j.nicl.2016.06.019>.
- McLeod, K.R., Langevin, L.M., Goodyear, B.G., Dewey, D., 2014. Functional connectivity of neural motor networks is disrupted in children with developmental coordination disorder and attention-deficit/hyperactivity disorder. *NeuroImage: Clin.* 4, 566–575. <https://doi.org/10.1016/j.nicl.2014.03.010>.

- Milner, A.D., Goodale, M.A., 2008. Two visual systems re-viewed. *Neuropsychologia* 46 (3), 774–785. <https://doi.org/10.1016/j.neuropsychologia.2007.10.005>.
- Mosca, S.J., Langevin, L.M., Dewey, D., Innes, A.M., Lionel, A.C., Marshall, C.C., Scherer, S.W., Parboosingh, J.S., Bernier, F.P., 2016. Copy-number variations are enriched for neurodevelopmental genes in children with developmental coordination disorder. *J. Med. Genet.* 53 (12), 812–819. <https://doi.org/10.1136/jmedgenet-2016-103818>.
- Muthukumaraswamy, S.D., Singh, K.D., 2011. A cautionary note on the interpretation of phase-locking estimates with concurrent changes in power. *Clin. Neurophysiol.* 122 (11), 2324–2325. <https://doi.org/10.1016/j.clinph.2011.04.003>.
- Myronenko, A., Song, X., 2010. Point Set Registration: Coherent Point Drift. *IEEE Trans. Pattern Anal. Mach. Intell.* 32 (12), 2262–2275. <https://doi.org/10.1109/TPAMI.2010.46>.
- Naeije, G., Wens, V., Coquelet, N., Sjøgård, M., Goldman, S., Pandolfo, M., De Tiège, X.P., 2020. Age of onset determines intrinsic functional brain architecture in Friedreich ataxia. *Ann. Clin. Transl. Neurol.* 7 (1), 94–104. <https://doi.org/10.1002/acn3.50966>.
- Nelson, H.E., 1976. A Modified Card Sorting Test Sensitive to Frontal Lobe Defects. *Cortex* 12 (4), 313–324. [https://doi.org/10.1016/S0010-9452\(76\)80035-4](https://doi.org/10.1016/S0010-9452(76)80035-4).
- Nichols, T.E., Holmes, A.P., 2002. Nonparametric permutation tests for functional neuroimaging: A primer with examples. *Hum. Brain Mapp.* 15 (1), 1–25. <https://doi.org/10.1002/hbm.1058>.
- Oldfield, R.C., 1971. The assessment and analysis of handedness: The Edinburgh inventory. *Neuropsychologia* 9 (1), 97–113. [https://doi.org/10.1016/0028-3932\(71\)90067-4](https://doi.org/10.1016/0028-3932(71)90067-4).
- Oostenveld, R., Fries, P., Maris, E., Schoffelen, J.-M., 2011. FieldTrip: Open Source Software for Advanced Analysis of MEG, EEG, and Invasive Electrophysiological Data. *Comput. Intell. Neurosci.* 2011, 1–9. <https://doi.org/10.1155/2011/156869>.
- Pang, E.W., Gaetz, W., Otsubo, H., Chuang, S., Cheyne, D., 2003. Localization of auditory N1 in children using MEG: Source modeling issues. *Int. J. Psychophysiol.* 51 (1), 27–35. [https://doi.org/10.1016/S0167-8760\(03\)00150-8](https://doi.org/10.1016/S0167-8760(03)00150-8).
- Pangelinan, M.M., Hatfield, B.D., Clark, J.E., 2013. Differences in movement-related cortical activation patterns underlying motor performance in children with and without developmental coordination disorder. *J. Neurophysiol.* 109 (12), 3041–3050. <https://doi.org/10.1152/jn.00532.2012>.
- Papeo, L., Lingnau, A., Agosta, S., Pascual-Leone, A., Battelli, L., Caramazza, A., 2015. The Origin of Word-related Motor Activity. *Cereb. Cortex* 25 (6), 1668–1675. <https://doi.org/10.1093/cercor/bht423>.
- Pascual-Marqui, R.D., 2002. Standardized low resolution brain electromagnetic tomography (sLORETA): technical details. *Methods Find Exp Clin Pharmacol* 16.
- Pearson, J.M., Heilbronner, S.R., Barack, D.L., Hayden, B.Y., Platt, M.L., 2011. Posterior cingulate cortex: Adapting behavior to a changing world. *Trends Cogn. Sci.* 15 (4), 143–151. <https://doi.org/10.1016/j.tics.2011.02.002>.
- Piek, J.P., Dyck, M.J., 2004. Sensory-motor deficits in children with developmental coordination disorder, attention deficit hyperactivity disorder and autistic disorder. *Hum. Mov. Sci.* 23 (3–4), 475–488. <https://doi.org/10.1016/j.humov.2004.08.019>.
- Price, A.R., Peelle, J.E., Bonner, M.F., Grossman, M., Hamilton, R.H., 2016. Causal Evidence for a Mechanism of Semantic Integration in the Angular Gyrus as Revealed by High-Definition Transcranial Direct Current Stimulation. *J. Neurosci.* 36 (13), 3829–3838. <https://doi.org/10.1523/JNEUROSCI.3120-15.2016>.
- Querre, L., Berquin, P., Vernier-Hauvette, M.-P., Fall, S., Deltour, L., Meyer, M.-E., de Marco, G., 2008. Dysfunction of the attentional brain network in children with Developmental Coordination Disorder: A fMRI study. *Brain Res.* 1244, 89–102. <https://doi.org/10.1016/j.brainres.2008.07.066>.
- Reynolds, J.E., Billington, J., Kerrigan, S., Williams, J., Elliott, C., Winsor, A.M., Codd, L., Bynevelt, M., Licari, M.K., 2019. Mirror neuron system activation in children with developmental coordination disorder: A replication functional MRI study. *Res. Dev. Disabil.* 84, 16–27. <https://doi.org/10.1016/j.ridd.2017.11.012>.
- Reynolds, J.E., Licari, M.K., Billington, J., Chen, Y., Aziz-Zadeh, L., Werner, J., Winsor, A.M., Bynevelt, M., 2015a. Mirror neuron activation in children with developmental coordination disorder: A functional MRI study. *Int. J. Dev. Neurosci.* 47 (Part B), 309–319. <https://doi.org/10.1016/j.ijdevneu.2015.10.003>.
- Reynolds, J.E., Licari, M.K., Elliott, C., Lay, B.S., Williams, J., 2015b. Motor imagery ability and internal representation of movement in children with probable developmental coordination disorder. *Hum. Mov. Sci.* 44, 287–298. <https://doi.org/10.1016/j.humov.2015.09.012>.
- Rinat, S., Izadi-Najafabadi, S., Zwicker, J.G., 2020. Children with developmental coordination disorder show altered functional connectivity compared to peers. *NeuroImage: Clin.* 27 (102309), 12. <https://doi.org/10.1016/j.nicl.2020.102309>.
- Rizzolatti, G., Matelli, M., 2003. Two different streams form the dorsal visual system: Anatomy and functions. *Exp. Brain Res.* 153 (2), 146–157. <https://doi.org/10.1007/s00221-003-1588-0>.
- Rodríguez-Martínez, E.I., Ruiz-Martínez, F.J., Barriga Paulino, C.I., Gómez, C.M., 2017. Frequency shift in topography of spontaneous brain rhythms from childhood to adulthood. *Cogn. Neurodyn.* 11 (1), 23–33. <https://doi.org/10.1007/s11571-016-9402-4>.
- Schott, B.H., Wüstenberg, T., Lücke, E., Pohl, I.-M., Richter, A., Seidenbecher, C.I., Pollmann, S., Kizilirmak, S.M., Richardson-Klavehn, A., 2019. Gradual acquisition of visuospatial associative memory representations via the dorsal precuneus. *Hum. Brain Mapp.* 40 (5), 1554–1570. <https://doi.org/10.1002/hbm.24467>.
- Seghier, M.L., 2013. The Angular Gyrus: Multiple Functions and Multiple Subdivisions. *Neuroscientist* 19 (1), 43–61. <https://doi.org/10.1177/1073858412440596>.
- Shallice, T., 1982. Specific impairments of planning. *Philos. Trans. Royal Soc. Lond. B Biol. Sci.* 298 (1089), 199–209. <https://doi.org/10.1098/rstb.1982.0082>.
- Sjøgård, M., De Tiège, X., Mary, A., Peigneux, P., Goldman, S., Nagels, G., van Schependom, J., Quinn, A.J., Woolrich, M.W., Wens, V., 2019. Do the posterior midline cortices belong to the electrophysiological default-mode network? *NeuroImage* 200, 221–230. <https://doi.org/10.1016/j.neuroimage.2019.06.052>.
- Sjøgård, M., Wens, V., Van Schependom, J., Costers, L., D'hooghe, M., D'haeseleer, M., Woolrich, M., Goldman, S., Nagels, G., De Tiège, X., 2021. Brain dysconnectivity relates to disability and cognitive impairment in multiple sclerosis. *Hum. Brain Mapp.* 42 (3), 626–643. <https://doi.org/10.1002/hbm.25247>.
- Smith, S.M., Fox, P.T., Miller, K.L., Glahn, D.C., Fox, P.M., Mackay, C.E., Filippini, N., Watkins, K.E., Toro, R., Laird, A.R., Beckmann, C.F., 2009. Correspondence of the brain's functional architecture during activation and rest. *Proc. Natl. Acad. Sci.* 106 (31), 13040–13045. <https://doi.org/10.1073/pnas.0905267106>.
- Sumner, E., Pratt, M.L., Hill, E.L., 2016. Examining the cognitive profile of children with Developmental Coordination Disorder. *Res. Dev. Disabil.* 56, 10–17. <https://doi.org/10.1016/j.ridd.2016.05.012>.
- Taulu, S., Simola, J., Kajola, M., 2005. Applications of the signal space separation method. *IEEE Trans. Signal Process.* 53 (9), 3359–3372. <https://doi.org/10.1109/TSP.2005.853302>.
- Thornton, S., Bray, S., Langevin, L.M., Dewey, D., 2018. Functional brain correlates of motor response inhibition in children with developmental coordination disorder and attention deficit/hyperactivity disorder. *Hum. Mov. Sci.* 59, 134–142. <https://doi.org/10.1016/j.humov.2018.03.018>.
- Tsai, C.-L., Chang, Y.-K., Hung, T.-M., Tseng, Y.-T., Chen, T.-C., 2012. The neurophysiological performance of visuospatial working memory in children with developmental coordination disorder: Visuospatial Working Memory in Children with DCD. *Dev. Med. Child Neurol.* 54 (12), 1114–1120. <https://doi.org/10.1111/j.1469-8749.2012.04408.x>.
- Tsai, C.-L., Wilson, P.H., Wu, S.K., 2008. Role of visual-perceptual skills (non-motor) in children with developmental coordination disorder. *Hum. Mov. Sci.* 27 (4), 649–664. <https://doi.org/10.1016/j.humov.2007.10.002>.
- Vaivre-Douret, L., Lalanne, C., Ingster-Moati, I., Bodaert, N., Cabrol, D., Dufier, J.-L., Golse, B., Falissard, B., 2011. Subtypes of Developmental Coordination Disorder: Research on Their Nature and Etiology. *Dev. Neuropsychol.* 36 (5), 614–643. <https://doi.org/10.1080/87565641.2011.560696>.
- Van Dyck, D., Coquelet, N., Deconinck, N., Aeby, A., Bajiot, S., Goldman, S., Urbain, C., Trotta, N., Wens, V., De Tiège, X., 2020. MEG and high-density EEG resting-state networks mapping in children. *Clin. Neurophysiol.* 131 (11), 2713–2715. <https://doi.org/10.1016/j.clinph.2020.09.003>.
- Van Dyck, D., Deconinck, N., Aeby, A., Bajiot, S., Coquelet, N., De Tiège, X., Urbain, C., Under review. Atypical procedural learning skills in children with Developmental Coordination Disorder: The critical control of ADHD symptoms.
- Van Dyck, D., Deconinck, N., Aeby, A., Bajiot, S., Coquelet, N., Trotta, N., Rovai, A., Goldman, S., Urbain, C., Wens, V., De Tiège, X., 2021. Resting-state functional brain connectivity is related to subsequent procedural learning skills in school-aged children. *NeuroImage* 240, 118368. <https://doi.org/10.1016/j.neuroimage.2021.118368>.
- Vigario, R., Sarela, J., Jousmiki, V., Hamalainen, M., Oja, E., 2000. Independent component approach to the analysis of EEG and MEG recordings. *IEEE Trans. Biomed. Eng.* 47 (5), 589–593. <https://doi.org/10.1109/10.841330>.
- Visser, J., 2003. Developmental coordination disorder: A review of research on subtypes and comorbidities. *Hum. Mov. Sci.* 22 (4–5), 479–493. <https://doi.org/10.1016/j.humov.2003.09.005>.
- Watson, D., Clark, L.A., Chmielewski, M., Kotov, R., 2013. The value of suppressor effects in explicating the construct validity of symptom measures. *Psychol. Assess.* 25 (3), 929–941. <https://doi.org/10.1037/a0032781>.
- Wechsler, D., 2016. Échelle d'intelligence de Wechsler pour enfants et adolescents, 5ème édition (WISC-V)—Adaptation française. *CEPA par Pearson*.
- Wens, V., Marty, B., Mary, A., Bourguignon, M., Op de Beeck, M., Goldman, S., Van Bogaert, P., Peigneux, P., De Tiège, X., 2015. A geometric correction scheme for spatial leakage effects in MEG/EEG seed-based functional connectivity mapping: Spatial Leakage Geometric Correction Scheme. *Hum. Brain Mapp.* 36 (11), 4604–4621. <https://doi.org/10.1002/hbm.22943>.
- Wens, V., Mary, A., Bourguignon, M., Goldman, S., Marty, B., Op de Beeck, M., Bogaert, P.V., Peigneux, P., De Tiège, X., 2014. About the electrophysiological basis of resting state networks. *Clin. Neurophysiol.* 125 (8), 1711–1713. <https://doi.org/10.1016/j.clinph.2013.11.039>.
- Wilson, P., Ruddock, S., Rahimi-Golkhandan, S., Piek, J., Sugden, D., Green, D., Steenbergen, B., 2020. Cognitive and motor function in developmental coordination disorder. *Dev. Med. Child Neurol.* 62 (11), 1317–1323. <https://doi.org/10.1111/dmcn.14646>.
- Wilson, P.H., Ruddock, S., Smits-engelsman, Bouwien, Polatajko, Helene, Blank, Rainer, 2013. Understanding performance deficits in developmental coordination disorder: A meta-analysis of recent research: Review. *Dev. Med. Child Neurol.* 55 (3), 217–228. <https://doi.org/10.1111/j.1469-8749.2012.04436.x>.
- Wolpert, D.M., Flanagan, J.R., 2001. Motor prediction. *Curr. Biol.* 11 (18), R729–R732. [https://doi.org/10.1016/S0960-9822\(01\)00432-8](https://doi.org/10.1016/S0960-9822(01)00432-8).
- Xia, M., Wang, J., He, Y., Csermely, P., 2013. BrainNet Viewer: A Network Visualization Tool for Human Brain Connectomics. *PLoS ONE* 8 (7), e68910. <https://doi.org/10.1371/journal.pone.0068910>.

- Zimmermann, P., Fimm, B., 2004. Tests d'évaluation de l'attention (TEA, version 1.6): Normes pour enfants et adolescents, Manuel supplémentaire. Psytest.
- Zwicker, J.G., Missiuna, C., Boyd, L.A., 2009. Neural Correlates of Developmental Coordination Disorder: A Review of Hypotheses. *J. Child Neurol.* 24 (10), 1273–1281. <https://doi.org/10.1177/0883073809333537>.
- Zwicker, J.G., Missiuna, C., Harris, S.R., Boyd, L.A., 2010. Brain Activation of Children With Developmental Coordination Disorder is Different Than Peers. *Pediatrics* 126 (3), e678–e686. <https://doi.org/10.1542/peds.2010-0059>.
- Zwicker, J.G., Missiuna, C., Harris, S.R., Boyd, L.A., 2011. Brain activation associated with motor skill practice in children with developmental coordination disorder: An fMRI study. *Int. J. Dev. Neurosci.* 29 (2), 145–152. <https://doi.org/10.1016/j.ijdevneu.2010.12.002>.